Author Manuscript

Author Manuscript

Author Manuscript

Author Manuscript

HHS Public Access

Author manuscript

Mol Cell. Author manuscript; available in PMC 2020 September 05.

Published in final edited form as:

Mol Cell. 2019 September 05; 75(5): 957–966.e8. doi:10.1016/j.molcel.2019.05.031.

Stresses that raise Np_4A levels induce protective nucleoside tetraphosphate capping of bacterial RNA

Daniel J. Luciano[1,2], **Rose Levenson-Palmer**[1,2], **Joel G. Belasco**[1,2,*]

[1]Kimmel Center for Biology and Medicine at the Skirball Institute, New York University School of Medicine, 540 First Avenue, New York, NY 10016, USA

[2]Department of Microbiology, New York University School of Medicine, 430 E. 29th Street, New York, NY 10016, USA

SUMMARY

Present in all realms of life, dinucleoside tetraphosphates (Np_4Ns) are generally considered signaling molecules. However, only a single pathway for Np_4N signaling has been delineated in eukaryotes, and no receptor that mediates the influence of Np_4Ns has ever been identified in bacteria. Here we show that, under disulfide stress conditions that elevate cellular Np_4N concentrations, diverse *Escherichia coli* mRNAs and sRNAs acquire a cognate Np_4 cap. Purified *E. coli* RNA polymerase and lysyl-tRNA synthetase are both capable of adding such 5′ caps. Cap removal by either of two pyrophosphatases, ApaH or RppH, triggers rapid RNA degradation in *E. coli*. ApaH, the predominant decapping enzyme, functions as both a sensor and an effector of disulfide stress, which inactivates it. These findings suggest that the physiological changes attributed to elevated Np_4N concentrations in bacteria may result from widespread Np_4 capping, leading to altered RNA stability and consequent changes in gene expression.

Graphical Abstract

*Corresponding author and Lead contact, joel.belasco@med.nyu.edu.

AUTHOR CONTRIBUTIONS

D.J.L., R.L.-P., and J.G.B. designed the experiments, D.J.L. and R.L.-P. conducted the experiments, and D.J.L., R.L.-P., and J.G.B. interpreted the data and wrote the paper.

DECLARATION OF INTERESTS

The authors declare no competing interests.

Publisher's Disclaimer: This is a PDF file of an unedited manuscript that has been accepted for publication. As a service to our customers we are providing this early version of the manuscript. The manuscript will undergo copyediting, typesetting, and review of the resulting proof before it is published in its final citable form. Please note that during the production process errors may be discovered which could affect the content, and all legal disclaimers that apply to the journal pertain.

Author Manuscript Author Manuscript Author Manuscript Author Manuscript

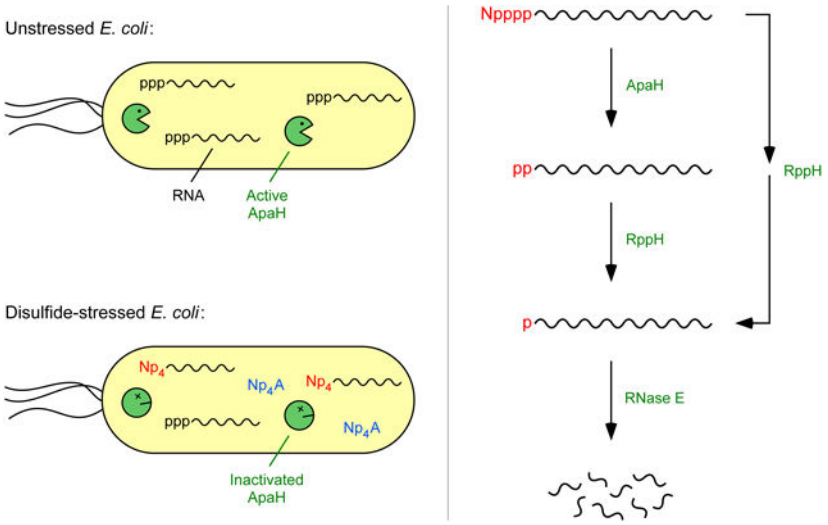

eTOC blurb

Luciano et al. report that disulfide stress induces nucleoside tetraphosphate (Np_4) capping of *E. coli* RNAs and that decapping can govern transcript lifetimes *in vivo*. Their findings suggest that physiological changes previously attributed to receptor-mediated Np_4A signaling may result instead from the impact of Np_4 capping on bacterial gene expression.

Keywords

Ap_4A; diadenosine tetraphosphate; RNA degradation; RNA decay; 5′ end; NCIN; aminoacyl-tRNA synthetase; LysU; esCAPade; boronate gel; cadmium; diamide; oxidative stress

INTRODUCTION

Since their discovery more than 50 years ago (Finamore and Warner, 1963; Zamecnik et al., 1966; Randerath et al., 1966), dinucleoside 5′,5′′-P^1,P^4-tetraphosphates (Np_4Ns) have attracted the interest of scientists seeking to elucidate their physiological roles and molecular function. Over the ensuing decades, they have been found in all realms of life, both prokaryotic and eukaryotic (Plateau and Blanquet, 1994; Kisselev et al., 1998), and, despite scant evidence as to their mechanism of action in any organism, have come to be regarded as signaling molecules. For example, in bacteria, where their concentration increases during oxidative stress and heat shock (Lee et al., 1983; Bochner et al., 1984; Coste et al., 1987), dinucleoside tetraphosphates are thought to act as alarmones, i.e. as second messengers for stress (Varshavsky, 1983). In eukaryotes, these molecules have been implicated in immune responses, neuronal signaling, and cardiovascular function (Boulos et al., 2016).

The dinucleoside tetraphosphates Ap_4A, Gp_4A, Cp_4A, and Up_4A are generated in cells as by-products of tRNA aminoacylation when the aminoacyl-adenylate intermediate reacts with a nucleoside triphosphate rather than with tRNA or pyrophosphate (Zamecnik et al., 1966; Randerath et al., 1966; Plateau and Blanquet, 1994), and their concentration in *E. coli* can be increased simply by overproducing any of several aminoacyl-tRNA synthetases (Brevet et

Author Manuscript Author Manuscript Author Manuscript Author Manuscript

al., 1989). Their cellular concentration is also elevated in bacterial mutants lacking RppH or ApaH, two enzymes that catalyze the hydrolysis of dinucleoside tetraphosphates to generate either an NTP and an NMP or two NDPs, respectively (Plateau et al., 1985; Farr et al., 1989; Lévêque et al., 1990; Cartwright et al., 1999). In addition to acting as an Np_4A hydrolase, RppH functions *in vivo* as an RNA pyrophosphohydrolase that converts the 5′-terminal triphosphate or diphosphate of bacterial transcripts to a monophosphate as a prelude to rapid RNA degradation by the 5′-monophosphate-stimulated endonuclease RNase E (Mackie, 1998; Deana et al., 2008; Luciano et al., 2017).

ApaH is the principal Np_4A hydrolase in proteobacteria, and deleting its gene leads not only to a marked increase in Np_4A levels but also to a variety of interesting phenotypes, including diminished motility, increased sensitivity to heat shock and oxidative stress, greater vulnerability to aminoglycosides, reduced antibiotic tolerance, impaired regulation of biofilm formation, disrupted coupling of DNA replication and cell division, and a decreased ability to invade mammalian cells (Farr et al., 1989; Johnstone and Farr, 1991; Nishimura et al., 1997; Ismail et al., 2003; Hansen et al., 2008; Monds et al., 2010; Ji et al., 2019). The correlation between these phenotypes and elevated Np_4A levels has widely been interpreted as evidence for signaling by these putative alarmones. However, for none of the phenotypic defects of Δ*apaH* mutants has the underlying molecular mechanism been determined. Moreover, no receptor that mediates the effects of dinucleoside tetraphosphates, a definitional requirement of second messengers, has ever been identified in bacteria. Even in eukaryotes, there is only a single instance in which a pathway for Np_4A signaling has been delineated (Lee et al., 2004).

This long-standing mystery raised the possibility that the primary biological function of Np_4As and the enzymes that hydrolyze them has been misunderstood. Here we report that, under conditions and in mutants that increase the cellular concentration of Np_4As, *E. coli* RNAs acquire a cognate nucleoside tetraphosphate (Np_4) cap and that the efficient degradation of these capped RNAs requires cap removal by ApaH. These findings suggest that the striking physiological changes heretofore attributed to receptor-mediated signaling by Np_4As may instead result from changes in bacterial gene expression caused by the impaired degradation of Np_4-capped transcripts.

RESULTS

Widespread RNA capping in cadmium-stressed cells

The structural similarity of dinucleoside tetraphosphates (N[5′]pppp[5′]N; Fig. 1A) to the capped 5′ end of eukaryotic mRNAs (m^7 G[5′]ppp[5′]N…) prompted us to examine whether increased Np_4A levels might be correlated in *E. coli* with the presence of mRNAs bearing a novel Np_4 cap. Cadmium stress elicits a particularly high concentration of Ap_4A, Gp_4A, Cp_4A, and Up_4A in this organism (220-950 μM) (Bochner et al., 1984; Coste et al., 1987), far above their concentration in unstressed cells (0.6-2.4 μM) (Plateau et al., 1987). Therefore, cadmium chloride was added to a log-phase *E. coli* culture, and the appearance of capped transcripts was investigated by testing *in vitro* for both the resistance of the 5′-terminal phosphates of cellular mRNA to removal by alkaline phosphatase and the reduced

Author Manuscript Author Manuscript Author Manuscript Author Manuscript

electrophoretic mobility of cellular transcripts through a matrix that selectively retards capped RNAs.

As a model, we chose the *E. coli yeiP* transcript, which encodes a paralog of translation elongation factor EF-P. When extracted from unstressed cells, the 5′ phosphates of *yeiP* mRNA were susceptible to removal by alkaline phosphatase, resulting in a hydroxylated 5′ end that was unreactive in a splinted-ligation assay (Fig. 1B; Fig. S1A) (Celesnik et al., 2007) (Luciano and Belasco, 2019). By contrast, 65% of the *yeiP* 5′ ends in RNA from cells subjected to cadmium stress were resistant to alkaline phosphatase and therefore ligatable after subsequent pyrophosphatase treatment to generate a monophosphorylated 5′ terminus, a finding suggestive of a 5′ cap.

The presence of a cap-like structure at this protected 5′ end was confirmed by the retarded mobility of 76% of *yeiP* mRNA from cadmium-stressed cells on a polyacrylamide gel containing boronate side chains that specifically reduce the electrophoretic mobility of transcripts bearing a vicinal diol characteristic of a 5′ cap (Fig. 1C) (Igloi and Kössel, 1985). By contrast, no low-mobility *yeiP* band was observed when the RNA was either decapped prior to boronate gel electrophoresis, examined by electrophoresis on an ordinary polyacrylamide gel, or extracted from unstressed cells. The mobility of capped *yeiP* mRNA from cadmium-stressed cells was indistinguishable on a boronate gel from that of *in vitro* transcribed *yeiP* RNA bearing an Ap_3, Ap_4, or Ap_5 cap but distinct from that of synthetic *yeiP* standards bearing an NAD or NADH cap (Fig. 1D, E). The capped mRNA from *E. coli* also co-migrated with *in vitro* transcripts bearing a Gp_4 or Up_4 cap but was slightly less mobile than a transcript bearing a Cp_4 cap (Fig. 1F). Together, these findings suggest that exposure of *E. coli* to cadmium causes most *yeiP* transcripts to acquire a nucleoside polyphosphate (Np_n) cap.

To test the generality of this phenomenon, we examined the 5′ end of 14 additional transcripts chosen at random, including protein-coding mRNAs and a non-coding sRNA. When extracted from cadmium-stressed *E. coli* cells, a substantial but variable fraction of each of these RNAs (median >40%) was found to migrate more slowly upon boronate gel electrophoresis (Table 1). Among them were capped transcripts confirmed by sequencing to begin with each of the four possible nucleotides (A, G, C, or U). None of the RNAs were detectably capped in unstressed cells (data not shown). By statistical extrapolation based on Bayes's rule for conditional probability, we calculate that a substantial majority of *E. coli* transcripts are likely to be capped to some extent in the presence of cadmium. The Npn caps induced by this stress appear to be much more ubiquitous and abundant in *E. coli* than NAD caps, which are found only on A-initiated transcripts and at low levels (typically <14% of 5′ ends (Cahová et al., 2015; Vvedenskaya et al., 2018)).

Decapping by ApaH and RppH

Many *E. coli* transcripts, including *yeiP* and *trxB* (thioredoxin reductase mRNA), are deprotected by enzyme-catalyzed conversion of the 5′ triphosphate to a monophosphate, thereby triggering RNA degradation (Deana et al., 2008; Richards et al., 2012; Luciano et al., 2017). By analogy, we tested three *E. coli* enzymes for their ability to decap Np_n-capped transcripts *in vitro*: two known to hydrolyze Np_4As (ApaH and RppH) and a third that

Author Manuscript Author Manuscript Author Manuscript Author Manuscript

removes nicotinamide mononucleotide from NAD-capped RNAs (NudC) (Guranowski et al., 1983; Plateau et al., 1985; Bessman et al., 2001; Cahová et al., 2015). ApaH and RppH were each able to efficiently decap both *yeiP* and *trxB* mRNA extracted from cadmium-stressed cells or synthesized with an Ap_4 or Gp_4 cap, whereas NudC was not (Fig. 2A; Fig. S2A). By contrast, only NudC and RppH were able to decap *in vitro* transcribed *yeiP* RNA bearing an NAD cap (Fig. S3). Although RppH has been shown to remove m^7 Gppp and NAD caps *in vitro* (Song et al., 2013; Cahová et al., 2015), ApaH has not previously been reported to have decapping activity.

To characterize the phosphorylation states of the products of decapping by ApaH and RppH, an Np_4-capped substrate – $Ap_4AG(CU)_{13}$ – bearing a single radiolabeled phosphate between the first and second transcribed nucleotides was synthesized *in vitro*. Alkaline hydrolysis of this capped RNA yielded Ap_4Ap as the predominant radiolabeled product, detectable by thin layer chromatography (Fig. 2B). Upon treatment of $Ap_4AG(CU)_{13}$ with purified ApaH or RppH, the principal radiolabeled product following alkaline hydrolysis was ppAp or pAp, respectively, results consistent with the products of Ap_4A hydrolysis by these enzymes (Guranowski et al., 1983; Plateau et al., 1985; Bessman et al., 2001). Radioactive products containing the same number of phosphates (ppGp or pGp) were obtained after decapping ^{32}P-labeled $Gp_4GA(CU)_{13}$ (Fig. 2B). These findings indicate that decapping of Np_4-capped RNA by ApaH generates a diphosphorylated RNA product, whereas decapping by RppH generates a monophosphorylated product, either directly or via a decapped intermediate bearing multiple 5′ phosphates.

Structural characterization of the RNA caps in cadmium-stressed cells

To definitively ascertain the structure of the RNA caps in cadmium-stressed *E. coli* cells, we first devised a method for determining the number of phosphates they contain. This method, called esCAPade (Enumeration of Shielded Cap-Associated Phosphates by Analysis of Decapped Ends), involves comparing the 5′ phosphorylation state of the products obtained by decapping cellular RNA and a set of Ap_n-capped standards with ApaH (Fig. S1). Ap_3, Ap_4, and Ap_5-capped *yeiP* standards synthesized by *in vitro* transcription and *yeiP* mRNA from *E. coli* cells exposed to cadmium chloride were each treated with alkaline phosphatase to remove the 5′ phosphates of any uncapped contaminants (Fig. S4A) and then with ApaH to release the cap. The phosphorylation state of the RNA products was subsequently analyzed by two methods: PABLO (Phosphorylation Assay By Ligation of Oligonucleotides), which quantifies the percentage of 5′ ends that are monophosphorylated on the basis of their ability to undergo splinted ligation to a DNA oligonucleotide (Fig. S1A), and PACO (Phosphorylation Assay by Capping Outcome), which quantifies the percentage of 5′ ends that are diphosphorylated on the basis of their susceptibility to capping by the *Schizosaccharomyces pombe* guanylyltransferase Pce1 (Fig. S1B) (Celesnik et al., 2007; Luciano et al., 2017; Luciano and Belasco, 2019). The products of ApaH-mediated decapping of *yeiP* mRNA from cadmium-stressed cells were 93 ± 5% diphosphorylated and 13 ± 1% monophosphorylated, very similar to the products of the Ap_4-capped *yeiP* standard (95 ± 2% diphosphorylated and 3 ± 2% monophosphorylated) (Fig. 3A; Fig. S4B, C; Tables S1-S6). By contrast, the ApaH reaction products for the Ap_3-capped standard were primarily monophosphorylated, while those for the Ap_5-capped

Author Manuscript Author Manuscript Author Manuscript Author Manuscript

standard appeared to be mostly triphosphorylated. From these measurements, we calculate that 98 ± 7% of the Np_n caps in cadmium-treated cells contain four phosphates (Fig. 3B; Table S6).

We next characterized the cap nucleobase by using thin-layer chromatography to identify the nucleotides released when ^{32}P-labeled bulk mRNA isolated from cadmium-treated cells was decapped *in vitro*. Decapping with purified ApaH generated ADP, CDP, GDP, and an unidentified product (Fig. 3C; Fig. S5), evidence for diverse Np_4 caps under these conditions. UDP may also have been produced but would have been obscured by a co-migrating phosphate contaminant. Decapping with RppH generated the corresponding NMPs (Fig. S5).

Potential mechanisms of cap acquisition

In principle, cellular transcripts could become Np_4-capped at the moment of synthesis if RNA polymerase is capable of initiating transcription with a dinucleoside tetraphosphate in place of a nucleoside triphosphate. (Note that Np_4A and Ap_4N are synonymous due to molecular symmetry.) Alternatively, they could acquire such a cap post-transcriptionally by a mechanism reminiscent of Np_4A synthesis if aminoacyl-tRNA synthetases are able to catalyze the reaction of aminoacyl-adenylates not only with the 5′ triphosphate of mononucleotides but also with the triphosphorylated 5′ end of polynucleotide transcripts (Fig. S6). The potential of each of these capping mechanisms was tested *in vitro*. Purified *E. coli* RNA polymerase proved able to incorporate Ap_4A at the 5′ end of nascent *yeiP* transcripts, as judged by the retarded electrophoretic migration of the resulting RNA on a boronate gel and its accelerated migration after RppH treatment (Fig. 4A). Likewise, the *E. coli* lysyl-tRNA synthetase LysU was able to cap triphosphorylated *yeiP* RNA in the presence of ATP and lysine (Fig. 4B). These findings demonstrate the feasibility of each of these possible mechanisms of cap acquisition.

Contributions of ApaH and RppH to RNA decapping and degradation in *E. coli*

To determine the impact of ApaH and RppH on Np_4 caps in *E. coli*, we first examined the effect of mutations that eliminated each protein. Even in the absence of stress, capped mRNA was abundant in *E. coli* cells lacking ApaH (Fig. 5A; Fig. S2B). Indeed, every transcript shown to be capped in cadmium-stressed cells was also capped, albeit to a lesser extent, in unstressed Δ*apaH* cells (Table 1), and the phosphate content, cap nucleobase, and enzymatic reactivity of individual capped transcripts present under those two conditions were much the same (Fig. 5B; Fig. S7). By contrast, Np_4-capped RNA was not detected in unstressed cells lacking RppH (Fig. 5A, Fig. S2B).

To quantify the relative contributions of ApaH and RppH to the decapping of Np_4-capped transcripts in *E. coli*, we used boronate gel electrophoresis to monitor the effect of deficiencies in either of these enzymes on the rate of disappearance of capped mRNA after blocking further RNA synthesis. These experiments were first performed under normal growth conditions to avoid the physiological complications of cadmium stress. Because unstressed wild-type cells do not contain detectable levels of Np_4-capped mRNA, we monitored the disappearance of capped transcripts after arresting transcription in cells which

Author Manuscript Author Manuscript Author Manuscript Author Manuscript

either lacked ApaH altogether or contained sufficiently little that a small amount of capped mRNA could still be detected. Cellular ApaH levels were controlled by expressing the *apaH* gene from an arabinose-inducible promoter. The half-life of capped *yeiP* mRNA increased from 2.3 ± 0.1 min in the presence of arabinose (cap removal by both ApaH and RppH) to 4.5 ± 0.1 min in the complete absence of ApaH (cap removal by RppH only) (Fig. 5C). Capped *yeiP* mRNA was lost even more slowly from cells that lacked both ApaH and RppH, where its half-life of 10.8 ± 0.6 min reflected only the rate of 5′-end-independent degradation. From these values, we calculate that, at this level of induction, decapping by ApaH is 1.7 ± 0.1 times faster than decapping by RppH. The disparity in the contributions of these two enzymes to decapping would likely be even greater in wild-type cells, where the absence of detectable Np_4-capped RNA implies that ApaH activity is much higher. Similar effects were observed for cap removal from *trxB* (Fig. S2C).

The dominant role of ApaH in decapping and the ability of RppH to swiftly convert the resulting 5′ diphosphates to monophosphates capable of accelerating endonucleolytic cleavage by RNase E (Luciano et al., 2017) suggest a decay pathway in which ApaH and RppH act consecutively to trigger the degradation of Np_4-capped RNAs in *E. coli*. If so, a null mutation in *rppH* should be epistatic to a null mutation in *apaH*. To test this prediction, we compared the aggregate stability of all forms of *yeiP* and *trxB* mRNA (capped and uncapped combined) in wild-type cells and isogenic derivatives lacking either or both of these pyrophosphatases. The effect of ApaH alone on the aggregate half-life of these mRNAs was substantial. As judged by electrophoresis on an ordinary polyacrylamide gel, the half-life of full-length *yeiP* mRNA increased from 1.4 ± 0.2 min in wild-type cells to 3.5 ± 0.2 min in Δ*apaH* cells (Fig. 5D), while that of *trxB* mRNA increased from 2.2 ± 0.1 min to 3.8 ± 0.1 min (Fig. S2D). By contrast, in a Δ*rppH* background, deleting the *apaH* gene did not further stabilize either of these mRNAs (aggregate half-life of 8-9 min for *yeiP* and >30 min for *trxB*, irrespective of the presence or absence of ApaH), a finding consistent with the sequential action of these two enzymes on capped 5′ ends in *E. coli*.

Induction of Np_4 capping by disulfide stress

The affinity of cadmium for thiols enables it to crosslink cysteine residues (Delalande et al., 2010). To determine whether cysteine crosslinking triggers RNA capping in cadmium-treated cells, we examined the 5′ end of *yeiP* and *trxB* mRNA in *E. coli* cells treated with diamide, a chemical reagent that specifically joins cysteine thiols to create disulfide bonds (Kosower and Kosower, 1995). By doing so, it induces disulfide stress, a type of oxidative stress in which indiscriminate cysteine crosslinking causes proteins to misfold and aggregate (Leichert et al., 2003; Müller et al., 2013) and cellular Ap_4A levels rise dramatically (Bochner et al., 1984). Upon exposure to diamide, extensive capping was again observed for both the *yeiP* and *trxB* transcripts (Fig. 6A; Fig. S2E). The similar effect of cadmium and diamide suggests that *E. coli* cells produce Np_4-capped RNA in response to disulfide stress.

To account for the abundance of Np_4-capped transcripts in disulfide-stressed cells, we investigated whether ApaH is inactivated by inducers of this stress. *In vitro*, the decapping activity of this enzyme is greatly diminished by treatment with either cadmium chloride or diamide (Fig. 6B), a finding consistent with a previous report that its Np_4A hydrolase

Author Manuscript Author Manuscript Author Manuscript Author Manuscript

activity is sensitive to sulfhydryl reagents (Guranowski et al., 1983). Moreover, in wild-type *E. coli* cells experiencing disulfide stress, the rate of *yeiP* and trxB decapping is very slow and is not further retarded by deleting the *apaH* gene (Figure 6C; Figure S2F), evidence that ApaH is inactivated under these conditions. Therefore, it appears that ApaH governs mRNA lifetimes by acting as both a sensor and an effector of disulfide stress induction.

DISCUSSION

Although dinucleoside tetraphosphates have long been thought to function as second messengers, their mechanism of action has largely resisted elucidation. In bacterial cells, where their concentration increases in reaction to stress, they have been deemed alarmones responsible for a variety of intriguing physiological changes, even though no receptor through which they signal has been identified. Our results now show that, during disulfide stress, a marked increase in Np_4A levels is accompanied by widespread Np_4 capping of *E. coli* transcripts and prolonged RNA lifetimes. Similar changes occur in cells lacking the principal Np_4A hydrolase ApaH. Consistent with these observations, ApaH appears to be the enzyme primarily responsible for removing Np_4 caps in *E. coli*, and it is inactivated by inducers of disulfide stress. In unstressed cells, decapping by ApaH can trigger rapid RNA degradation. This decay pathway is blocked by ApaH inactivation in disulfide-stressed cells.

In *E. coli* cells experiencing disulfide stress or lacking ApaH, Np_4 caps have been detected at a variable level on every transcript tested, including protein-coding and noncoding RNAs and RNAs that begin with A, G, C, or U (Table 1). For reasons that are not yet apparent, the highest levels of capping are observed on A-, C-, or U-initiated transcripts (26-76% capped in cadmium-stressed cells), while the lowest levels are found on G-initiated transcripts (4-8%). Transcript-specific differences in cap levels are likely to have many causes. They reflect disparities not only in the efficiency of capping and decapping but also in the rate of subsequent RNA breakdown, as some of the uncapped RNA detected under these conditions undoubtedly has already been decapped as a prelude to degradation. Consequently, the steady-state percentage of a particular transcript that is capped represents not the total fraction that is capped at some point during the lifetime of the transcript but rather a lower limit on that fraction. Consistent with this interpretation is the substantial effect of ApaH on the aggregate decay rate of *yeiP* and *trxB* mRNA despite the modest percentage of these transcripts that remains capped at any particular moment in Δ*apaH* cells (19-36%). Therefore, the absence of detectable Np_4-capped RNA in unstressed wild-type cells could signify either that very little of it forms under those conditions or that it is decapped by ApaH too quickly for the capped RNA to accumulate appreciably.

In principle, *E. coli* RNAs could acquire Np_4 caps either by incorporating dinucleoside tetraphosphates at the 5′ end of nascent transcripts during transcription initiation or by a post-transcriptional mechanism such as that employed by aminoacyl-tRNA synthetases to produce Np_4As from NTPs (Zamecnik et al., 1966; Brevet et al., 1989; Fraga and Fontes, 2011). The former mechanism would be consonant with evidence that *E. coli* RNA polymerase can initiate transcription with noncanonical nucleotides (Bird et al., 2016), while the latter would implicate an important class of enzymes known for charging the 3′ end of tRNAs in modifying the triphosphorylated 5′ end of mRNAs and sRNAs so as to affect their

Author Manuscript Author Manuscript Author Manuscript Author Manuscript

degradation. Our *in vitro* tests with *E. coli* RNA polymerase and lysyl-tRNA synthetase demonstrate the feasibility of each of these cap acquisition mechanisms. The actual contributions of these or other mechanisms to Np_4 capping in *E. coli* will require validation *in vivo*.

Under ordinary growth conditions, the swift removal of Np_4 caps by ApaH generates a diphosphorylated 5′ end that can quickly be converted by RppH to a 5′ monophosphate, thereby enabling rapid RNA degradation by the endonuclease RNase E, which preferentially cleaves monophosphorylated RNAs (Mackie, 1998; Luciano et al., 2017). However, the inactivation of ApaH by inducers of disulfide stress impedes the deprotection and decay of Np_4-capped RNAs, allowing them to accumulate. RppH too can decap such transcripts, albeit more slowly, apparently releasing the cap as a nucleoside monophosphate to generate a triphosphorylated RNA 5′ end susceptible to subsequent RppH-dependent conversion to a 5′ monophosphate and further decay. By contrast, ApaH is not reactive with triphosphorylated RNA 5′ termini (data not shown). Despite its subordinate role in Np_4 cap removal, RppH has a greater impact than ApaH on the aggregate longevity of individual cellular transcripts, presumably because only RppH can trigger rapid RNase E-mediated degradation by completing the conversion of the 5′ end to a monophosphate.

The number of phosphates present in the 5′ caps observed during disulfide stress and in Δ*apaH* mutants was determined by esCAPade, a method devised for this purpose but applicable more generally. This assay takes advantage of the regioselectivity of decapping by ApaH, which releases the cap primarily as a nucleoside diphosphate regardless of the number of bridging phosphates originally associated with it. As a result, the number of phosphates in the 5′ cap of any ApaH-reactive RNA detectable by Northern blotting can be deduced by using established assays (PABLO and PACO (Luciano and Belasco, 2019)) to determine how many phosphates remain on the RNA 5′ end after cap removal by purified ApaH. Unlike some other possible approaches for examining the 5′ terminus of complex mixtures of cellular RNAs, such as mass spectrometry, esCAPade is quantitative and transcript-specific.

Disulfide stress, the physiological strain that causes Np_4 capping to become widespread in *E. coli*, is a condition that pathogenic bacteria may experience when engulfed by host phagocytes into the highly oxidizing environment of phagolysosomes (Åslund and Beckwith, 1999; Beavers and Skaar, 2016) or when exposed to cadmium in the environment (Hossain et al., 2012; Müller et al., 2013). Disulfide bond formation in several bacterial transcription factors, such as OxyR, is known to directly regulate their activity (Zheng et al., 1998; Antelmann and Helmann, 2011). Our discovery that the cysteine-containing decapping enzyme ApaH functions as both a sensor and an effector of disulfide stress indicates that disulfide bond formation can directly impact gene expression at the post-transcriptional level as well. Indeed, among the ApaH targets that become extensively capped and stabilized in response to disulfide stress is *trxB* mRNA, whose concentration increases in such cells (Helbig et al., 2008) and whose protein product (thioredoxin reductase) should help to ameliorate that stress (Müller et al., 2013). Further investigation will be needed to determine the impact of Np_4 capping on the recovery of *E. coli* from disulfide stress.

Author Manuscript Author Manuscript Author Manuscript Author Manuscript

For decades, the mechanism by which dinucleoside tetraphosphates fulfill their putative role as second messengers in cellular responses to stress has remained an enigma, particularly in bacteria, where no receptor that mediates their influence has been identified. Our discovery (i) that RNAs bearing a novel Np_4 cap are widespread in *E. coli* under the same conditions that elevate Np_4A levels and (ii) that the lifetimes of these RNAs are prolonged when ApaH is not able or available to decap them suggests that the many intriguing physiological changes previously attributed to Np_4A signaling via a hypothetical receptor may well result instead from altered patterns of bacterial gene expression caused by the impaired degradation of Np_4-capped RNAs. Elevated Np_4A levels may have similar consequences for capping in eukaryotic cells.

STAR METHODS

EXPERIMENTAL MODEL AND SUBJECT DETAILS

Np_4 capping and decapping were examined in *E. coli* cells during exponential growth and disulfide stress and *in vitro* with purified transcripts and proteins.

METHOD DETAILS

Strains and plasmids—Analysis of the 5′ end and decay rate of mRNA was performed in the *E. coli* K-12 strain BW25113 (Datsenko and Wanner, 2000) and isogenic derivatives thereof bearing in-frame deletions of the *apaH, rppH, araE*, or *araH* coding region, either individually or in combination. Each chromosomal deletion mutant was constructed by P1 transduction with the corresponding *kan*-disrupted gene from the Keio collection (Baba et al., 2006) followed by excision of the *kan* gene. In addition, the strains used to analyze *yeiP* mRNA contained plasmid pYeiP1 (Richards et al., 2012) to facilitate detection of that mRNA by increasing its cellular concentration, and the strain used to analyze *yeiP*-A1G mRNA lacked the chromosomal *yeiP* gene and contained plasmid pYeiP1-A1G. Finally, the strain used as a source of cellular RNA into which *in vitro* transcribed *trxB* RNA was spiked lacked the chromosomal *trxB* gene (Richards et al., 2012).

Two plasmids were used to test for complementation of the chromosomal Δ*apaH* allele. Plasmid pPlacApaH is a derivative of pPlacRppH (Deana et al., 2008) that encodes wild-type *E. coli* ApaH under the control of an IPTG-inducible *lac*UV5 promoter. A variant encoding catalytically inactive ApaH (pPlacApaH-D37A) was constructed from pPlacApaH by introducing a codon substitution (GAT → GCT) at position 37. Plasmid pPM30-araE is a derivative of pPM30 (Meacock and Cohen, 1980) that expresses AraE constitutively under the control of a *bla* promoter. Plasmid pPBAD-ApaH30 is a derivative of pPM30-araE that additionally encodes AraC and expresses ApaH under the control of an arabinose-inducible P_{BAD} promoter.

ApaH was purified from *E. coli* containing plasmid pET-ApaH or pET-ApaH-D37A, derivatives of pET28a(+) that encode *E. coli* ApaH or ApaH-D37A bearing a carboxy-terminal hexahistidine tag (GHHHHHH). RppH was purified from *E. coli* containing pPlacRppH6 or pPlacRppH6-E53A, plasmids that encode *E. coli* RppH or RppH-E53A bearing an amino-terminal hexahistidine tag (MHHHHHHG) (Deana et al., 2008). NudC

Author Manuscript Author Manuscript Author Manuscript Author Manuscript

was purified from *E. coli* containing plasmid pET-NudC or pET-NudC-E178A, derivatives of pET28a(+) that encode *E. coli* NudC or NudC-E178A bearing a carboxy-terminal hexahistidine tag (GHHHHHH). LysU was purified from *E. coli* containing pPlacLysU, a derivative of pPlacRppH6 that encodes *E. coli* LysU bearing an amino-terminal hexahistidine tag (MHHHHHHG).

Conditions for cell growth and disulfide stress induction—In most cases, cells were grown to mid-log phase (OD_{650} = 0.3) at 37°C in MOPS-glucose medium (Neidhardt et al., 1974) before harvesting RNA or inducing disulfide stress. Disulfide stress was induced by adding either $CdCl_2$ (0.2 mM) or diamide (2 mM), and RNA was harvested 90 min later. The cadmium-contaminated culture medium was subsequently disposed of as hazardous waste. To test for complementation of the Δ*apaH* allele, ApaH synthesis from plasmid pPlacApaH was enabled by growth in MOPS-glucose medium containing isopropyl-β-D-1-thiogalactopyranoside (IPTG) (1 mM). To examine the contributions of ApaH and RppH to rates of decapping in *E. coli*, isogenic strains containing plasmid pPBAD-ApaH30 or pPM30-araE were grown to mid-log phase (OD_{650} = 0.3) at 37°C in LB medium and then treated for 30 min with L-arabinose (0.2% v/v) to induce ApaH synthesis in the strain containing plasmid pPBAD-ApaH30.

RNA extraction from *E. coli*—Total cellular RNA was extracted from liquid cultures of *E. coli* as follows. A culture sample (10-15 ml) was rapidly chilled by pipetting it into a 50-ml centrifuge tube filled with crushed ice, and the bacteria were pelleted by centrifugation at 6,000 x *g* for 10 min at 0°C. The cell pellet was resuspended at 0°C in 125 μl of ice-cold buffer A (0.3 M sucrose, 10 mM sodium acetate, pH 4.5, 10 mM EDTA), transferred to a chilled microfuge tube, mixed with 250 μl of room-temperature buffer B (2% SDS, 10 mM sodium acetate, pH 4.5), and heated to 75°C for 3 min to lyse the cells. The cell lysate was extracted three times with 250 μl of hot, unneutralized, water-saturated phenol by vigorously agitating the mixture and then heating it to 75°C for 3 min. After each phenol extraction, the mixture was chilled rapidly in a dry ice/ethanol bath and then centrifuged at 21,000 x *g* for 5 min before transferring the aqueous layer to a new microfuge tube. Finally, the RNA was precipitated by mixing the aqueous layer of the last phenol extraction (up to 450 μl) with 3 M sodium acetate, pH 4.8 (45 μl) and ethanol (1 ml), cooled to – 20°C for 30 min, pelleted by centrifugation at 21,000 x *g* for 15 min, washed with 70% ethanol, air-dried, dissolved in water (30-70 μl) to a concentration of 0.5-2.0 μg/μl, and stored at −20°C.

Detection and quantification of capped RNA—Capped RNA was detected by boronate gel electrophoresis and Northern blotting after site-specific RNA cleavage 48-152 nt from the 5′ end with a 10-23 deoxyribozyme (Table S7) (Luciano and Belasco, 2019). The RNA was first annealed to a transcript-specific 10-23 deoxyribozyme (400 pmol) (Santoro and Joyce, 1997) in water by heating the mixture (36 μl) to 85°C for 5 min and then cooling it slowly to 30°C. A solution (4 μl) containing Tris-HCl, pH 7.5 (500 mM), $MgCl_2$ (100 mM), and dithiothreitol (10 mM) was then added, and RNA cleavage was allowed to proceed for 2 hr at 37°C. The reaction was quenched with EDTA (195 μl of a 4 mM solution), and the products were ethanol precipitated and subjected to electrophoresis on a denaturing gel containing 5.6% acrylamide:bisacrylamide (19:1), 0.25% 3-

Author Manuscript Author Manuscript Author Manuscript Author Manuscript

acrylamidophenylboronic acid (Ivanov et al., 2004), 7 M urea, and 0.1 M Tris-acetate, pH 9.0. Finally, the gel was electroblotted onto a nylon membrane, and the blot was probed with a ^{32}P-labeled oligonucleotide complementary to the RNA of interest. The percentage of the transcript that was capped was calculated from the ratio of band intensities (capped versus uncapped).

Alternatively, capped *yeiP* mRNA was detected on the basis of its resistance to 5′ phosphate removal by alkaline phosphatase, as follows. Total RNA (10 μg) extracted from *E. coli* BW25113 cells that had been exposed for 90 min to $CdCl_2$ (0 or 0.1 mM) was treated for 1 hr at 37°C with calf intestinal alkaline phosphatase (10 units) in a solution (20 μl) containing Tris-HCl, pH 7.9 (100 mM), NaCl (100 mM), $MgCl_2$ (10 mM), and dithiothreitol (1 mM). The reaction was quenched with EDTA (210 μl of a 3.5 mM solution), and the RNA was recovered by phenol extraction and ethanol precipitation and then treated for 2 hr at 37°C with tobacco acid pyrophosphatase (2 units) in a solution (20 μl) containing sodium acetate, pH 6.0 (50 mM), EDTA (1 mM), β-mercaptoethanol (0.1%), and Triton X-100 (0.01%). The RNA was recovered by phenol extraction and ethanol precipitation, and the percentage of *yeiP* 5′ ends that were monophosphorylated was determined by their ability to undergo splinted ligation to a DNA oligonucleotide in the presence of T4 DNA ligase and a bridging oligonucleotide complementary to both the first oligonucleotide and the 5′ end of *yeiP* mRNA (Table S7) (Luciano and Belasco, 2019).

RNA synthesis by *in vitro* transcription—Triphosphorylated, diphosphorylated, and monophosphorylated *yeiP* and *trxB* RNA was synthesized by *in vitro* transcription of DNA templates bearing a T7 ϕ2.5 promoter and a T→G substitution at the second transcribed position to enable efficient RNA synthesis by T7 RNA polymerase (Luciano et al., 2017). Their capped counterparts were synthesized by *in vitro* transcription in the presence of AP_3A, AP_4A, Ap_5A, GP_4A, CP_4A, UP_4A, NAD, or NADH at a concentration (1.5 mM) well in excess of ATP (0.25 mM). The resulting transcripts were purified by gel electrophoresis and elution of the band of interest.

Triphosphorylated, diphosphorylated, and monophosphorylated $AG(CU)_{13}$ and $GA(CU)_{13}$ bearing a ^{32}P-labeled phosphate between the first and second nucleotide were synthesized by *in vitro* transcription with T7 RNA polymerase in the presence of [α-^{32}P] GTP and either ATP, ADP, or AMP or in the presence of [α-^{32}P] ATP, and either GTP, GDP, or GMP, respectively (Deana et al., 2008). Ap_4-capped $AG(CU)_{13}$ and Gp_4-capped $GA(CU)_{13}$ were synthesized in a similar manner but in the presence of AP_4A (1.2 mM) or GP_4G (1.2 mM), respectively. The resulting transcripts were purified by gel electrophoresis and elution of the band of interest.

Analysis of capped 5′ ends by RACE—To confirm the identity of the first transcribed nucleotide of individual capped transcripts in *E. coli*, total RNA was extracted from wild-type cells that had been treated for 90 min with $CdCl_2$ (0.2 mM). The RNA samples (5 μg) were first treated with calf intestine alkaline phosphatase (10 units) for 1 hr at 37°C in a solution (20 μl) containing Tris-HCl, pH 7.9 (100 mM), NaCl (100 mM), $MgCl_2$ (10 mM), dithiothreitol (1 mM), and rRNasin (2 units/μl to convert uncapped 5′ ends to unligatable hydroxyls. The capped 5′ ends were subsequently converted to monophosphates by

Author Manuscript Author Manuscript Author Manuscript Author Manuscript

treatment with RppH (200 nM) for 2 hr at 37°C in a solution (20 μl) containing HEPES, pH 7.6 (20 mM), $MgCl_2$ (10 mM), dithiothreitol (1 mM), and rRNasin (2 units/μl). The decapped RNA was then ligated to a chimeric DNA-RNA oligonucleotide (RACE 1; Table S7) by treatment with T4 RNA ligase (5 units) for 2 hr 37°C in a solution (25 μl) containing Tris-HCl, pH 7.5 (50 mM), $MgCl_2$ (10 mM), dithiothreitol (1 mM), rRNasin (1 unit/μl), RACE 1 (1 μg), and ATP (1 mM). The ligation products were reverse transcribed by treatment with Superscript III reverse transcriptase (300 units) and a transcript-specific primer (5 pmol; Table S7) for 1 hr at 55°C in a solution (20 μl) containing Tris-HCl, pH 8.3 (50 mM), KCl (75 mM), $MgCl_2$ (3 mM), dithiothreitol (5 mM), dNTPs (0.5 mM each), and rRNasin (1 unit/μl), and the resulting cDNA was amplified by successive rounds of PCR with nested pairs of primers surrounding the transcription initiation site (Table S7). Finally, the PCR products were purified by agarose gel electrophoresis and sequenced.

Protein purification—*E. coli* ApaH, ApaH-D37A, RppH, RppH-E53A, NudC, NudC-E178A, and LysU and *Schizosaccharomyces pombe* Pce1, each bearing a terminal hexahistidine tag, were overproduced in *E. coli* BL21 (DE3) *rne*-131 Δ*rna* containing plasmid pET-ApaH, pET-ApaH-D37A, pPlacRppH6 (Deana et al., 2008), pPlacRppH6-E53A, pET-NudC, pET-NudC-E178A, pPlacLysU, or pSMT3-Pce1 (Doamekpor et al., 2014), respectively, and purified by affinity chromatography on TALON beads. Hexahistidine-tagged T4 DNA ligase was purified from *E. coli* strain MIC2067 (Itaya et al., 1999) containing plasmid pPlacT4L (Luciano et al., 2017) by affinity chromatography on TALON beads followed by anion-exchange chromatography on an UNO Q1 column.

RNA decapping by purified ApaH, RppH, and NudC—Total RNA (10 μg) from either $CdCl_2$-stressed wild-type *E. coli* cells or unstressed *E. coli* Δ*apaH* cells was treated with active or catalytically inactive forms of ApaH, RppH, or NudC (50 nM) for 5 min at 37°C in a solution (20 μl) containing HEPES, pH 7.6 (20 mM), $MgCl_2$ (5-10 mM), dithiothreitol (1 mM), and glycerol (1% v/v). Alternatively, Ap_4-, Gp_4-, or NAD-capped *yeiP* or *trxB* RNA (5 ng) synthesized by *in vitro* transcription was combined with total RNA (10 μg) from *E. coli* cells devoid of the corresponding transcript and treated similarly. In each case, the reaction was quenched with EDTA (210 μl of a 3.5 mM solution), and the products were phenol extracted, ethanol precipitated, cut with a 10-23 deoxyribozyme (DZyeiP69 or DZtrxB95) specific for *yeiP* or *trxB* mRNA, respectively, and analyzed by boronate gel electrophoresis and Northern blotting with a 5′ end-labeled oligonucleotide probe complementary to the RNA of interest.

Products of decapping by ApaH and RppH—Equal amounts (4,000 cpm) of Ap_4-capped $AG(CU)_{13}$ or Gp_4-capped $GA(CU)_{13}$ bearing a ^{32}P-labeled phosphate between the first and second transcribed nucleotide were decapped with purified ApaH or RppH (200 nM), as described above. The reaction was quenched by adding EDTA (5 μl of a 100 mM solution). A sample (10 μl) was removed, and the integrity of the RNA was examined by electrophoresis on a boronate gel prepared with 16% acrylamide:bisacrylamide (19:1) and 0.25% 3-acrylamidophenylboronic acid in 0.1 M Tris-acetate, pH 9.0, and 7 M urea. The remaining reaction product (15 μl) was subjected to alkaline hydrolysis by adding 0.2 M NaOH (5 μl) and heating the mixture at 95°C for 15 min. The hydrolysis products were

Author Manuscript Author Manuscript Author Manuscript Author Manuscript

neutralized with 3 M formic acid (5 μl) and spotted onto a PEI-cellulose TLC plate beside a set of markers generated by alkaline hydrolysis of untreated triphosphorylated, diphosphorylated, monophosphorylated, and Ap_4-capped $AG(CU)_{13}$ or triphosphorylated, diphosphorylated, monophosphorylated, and Gp_4-capped $GA(CU)_{13}$. The plate was developed with a solution containing 0.4 M ammonium sulfate, pH 5.5, and the radiolabeled spots were detected with a Typhoon Trio imager (GE Healthcare).

esCAPade—To determine the number of phosphates between the cap nucleoside and the first transcribed nucleoside of capped RNA, total RNA extracted either from wild-type *E. coli* cells that had been treated with 0.2 mM $CdCl_2$ for 90 minutes or from unstressed *E. coli* Δ*apaH* cells (10 μg) was analyzed in parallel with Ap_3-, Ap_4-, and Ap_5-capped *yeiP* RNA standards that had been synthesized by *in vitro* transcription (5 ng spiked into 10 μg of total RNA from *E. coli* Δ*yeiP* cells). All samples were analyzed in triplicate, including biological replicates of the cellular RNA. To convert any uncapped 5′ ends to unreactive hydroxyls, the RNA samples (10 μg) were first treated with calf intestine alkaline phosphatase (10 units) for 1 hr at 37°C in a solution (20 μl) containing Tris-HCl, pH 7.9 (100 mM), NaCl (100 mM), $MgCl_2$ (10 mM), dithiothreitol (1 mM), and rRNasin (2 units/μl). The reactions were quenched with EDTA (215 μl of a 3.5 mM solution), and the RNA was recovered by phenol extraction and ethanol precipitation. Next, the RNA samples were decapped with ApaH (200 nM) for 2 hours at 37°C in a solution (20 μl) containing of HEPES, pH 7.6 (20 mM), $MgCl_2$ (5 mM), dithiothreitol (1 mM), and rRNasin (2 units/μl). The reactions were quenched with EDTA (215 μl of a 3.5 mM solution), and the RNA was recovered by phenol extraction and ethanol precipitation. The RNA samples were then analyzed by PACO and PABLO (Fig. S1) to quantify the fraction of the decapped *yeiP* 5′ ends that were diphosphorylated (able to be recapped by *Schizosaccharomyces pombe* Pce1) or monophosphorylated (able to undergo splinted ligation by T4 DNA ligase), respectively (Luciano and Belasco, 2019). As standards for comparison, triphosphorylated, diphosphorylated, and monophosphorylated *yeiP* RNAs that had been synthesized by *in vitro* transcription and spiked into total RNA from *E. coli* Δ*yeiP* cells were analyzed in parallel. The resulting Northern blots were probed with a 5′ end-labeled oligonucleotide complementary to *yeiP* mRNA. Bands were visualized on a Typhoon Trio imager (GE Healthcare) and quantified by using ImageQuant TL software.

Characterization of the cap nucleobase—Wild type or Δ*apaH* cells were grown to mid-log phase (OD_{650} = 0.4) at 37°C in MOPS-glucose medium containing a low concentration of potassium phosphate (0.2 mM). Cells from a sample of the culture (25 ml) were pelleted by centrifugation, washed by resuspension in MOPS-glucose medium lacking potassium phosphate (25 ml), pelleted again, and resuspended in phosphate-free MOPS-glucose medium (14 ml). To half of the cells, ^{32}P-labeled orthophosphate (15 mCi, 0.18 μM) was added; to the other half, unlabeled potassium phosphate (0.18 μM) was added. (The unlabeled half was processed in parallel to help monitor the efficacy of disulfide stress and the progress of RNA purification and decapping.) After 5 min, the wild-type cells were treated with $CdCl_2$ (1 mM) for 90 min, and total RNA was extracted. Alternatively, total RNA was extracted from the Δ*apaH* cells without $CdCl_2$ treatment after radiolabeling them for 20 min. To convert uncapped 5′ ends to hydroxyls and hydrolyze any contaminating

Author Manuscript Author Manuscript Author Manuscript Author Manuscript

mononucleotides, the RNA samples (~150 μg) were first treated with calf intestine alkaline phosphatase (150 units) for 1 hr at 37°C in a solution (200 μl) containing Tris-HCl, pH 7.9 (50 mM), NaCl (100 mM), $MgCl_2$ (10 mM), bovine serum albumin (100 μg/ml), and rRNasin (2 units/μl). The reactions were quenched with EDTA and extracted with phenol, and the RNA was recovered by ethanol precipitation with ammonium acetate and fractionated on a 5%-to-25% sucrose gradient by centrifugation in an SW40 rotor for 23 hr at 35,000 rpm. Intermediate fractions that contained little or no rRNA or tRNA (as determined by polyacrylamide gel electrophoresis) were pooled, and the RNA in these fractions was recovered by ethanol precipitation with ammonium acetate. Any remaining mononucleotides were removed by gel filtration through Sephadex G-25 (1 ml, elution with water), and the RNA fractions were pooled, ethanol precipitated with ammonium acetate, and redissolved in water (80 μl). Samples of the RNA (10 μl) were then decapped or mock-treated either with ApaH (200 or 0 mM) for 30 min at 37°C in a solution (20 μl) containing HEPES, pH 7.6 (20 mM) and rRNAsin (1 unit/μl) or with RppH (200 or 0 mM) for 30 min at 37°C in a solution (20 μl) containing HEPES, pH 7.6 (20 mM), $MgCl_2$ (10 mM), and rRNAsin (1 unit/μl). The enzymes were inactivated by heating the reactions to 65°C for 10 min, and the reaction products were loaded directly onto a Sephadex G-25 column (1 ml) and eluted with water (100 μl fractions) to separate mononucleotides from RNA. The fractions containing mononucleotides were vacuum concentrated, and equal amounts (cpm) were mixed with unlabeled mononucleotide standards and analyzed by thin-layer chromatography on fluorescent PEI-cellulose plates developed with a buffer containing 0.4 M potassium phosphate, pH 3.3, and 5 mM EDTA. Radioactivity was detected with a Typhoon Trio imager (GE Healthcare), and the nucleotide standards were detected by UV quenching.

Cap incorporation by *E. coli* RNA polymerase—The 222-bp DNA template for *in vitro* transcription by *E. coli* RNA polymerase comprised a σ^{70} promoter and transcribed region derived from the *E. coli yeiP* gene (CTTAAGGTTAACCACCGAATTCATGAGCGCGCACAGTACCACCTTTTTTGCACCAGCAAAAGTGCGAATACCACTTGACAGAAAGGCCCGTCGCGAGTACTTTGTCGCG<u>ATATTTTTAACATTTTCGACTACAGGAATTTTTCGATGCCAAGAGCGAACGAAATTAAAAAAGGTATGGTACTGAATTACAACGGCTCGTATCCATATCGAAGAACGCAAAAA</u>, where the region encoding RNA is underlined). To facilitate transcription, the −35 region of the *yeiP* promoter was changed from TTGCCC to TTGACA. The 113-bp transcribed region of the template encoded the first 86 nt of *yeiP* mRNA (with a G → A substitution at position +9) fused to a 27-nt deoxyribozyme binding site.

Purified *E. coli* RNA polymerase holoenzyme (1 pmol, kindly provided by Venu Kamarthapu) was combined with the gel-purified DNA template (1 pmol) and incubated for 5 min at 37°C in a solution (10 μl) containing Tris-HCl, pH 8.0 (40 mM), NaCl (50 mM), and $MgCl_2$ (10 mM). A solution (1 μl) containing ATP (10 mM), UTP (2.5 mM), and AP_4A (0 or 50 mM) was added, and nascent transcripts were allowed to form for 5 min at 37°C. To radiolabel the RNA at positions +11 and +17, [α-^{32}P] CTP (4 μCi) was added, and the reaction mixture was left at room temperature for 5 min. Run-off transcription of the DNA template was then completed by adding a solution (2 μl) containing CTP, GTP, and UTP

Author Manuscript Author Manuscript Author Manuscript Author Manuscript

(333 μM each) and allowing RNA synthesis to continue for 5 min at room temperature. The reaction was quenched with EDTA (2 μl of a 120 mM solution), and the enzyme was heat-inactivated by incubation at 70°C for 20 min. The 3′ vicinal diol of the transcript was removed by site-specific cleavage with the 10-23 deoxyribozyme DZyeiP573 (4 μl of a 100 μM solution) in the presence of $MgCl_2$ (2 μl of a 220 mM solution) for 2 hr at 37°C. The cleavage reaction was quenched with EDTA (210 μl of a 3.5 mM solution), and the RNA was recovered by phenol extraction and ethanol precipitation. As a control, a portion of each reaction product was subsequently decapped by treatment with excess RppH (200 nM) for 2 hr at 37°C in a solution (20 μl) containing HEPES, pH 7.6 (20 mM), $MgCl_2$ (10 mM), dithiothreitol (1 mM), and rRNasin (2 units/μl). The radioactive products were then subjected to boronate gel electrophoresis and detected with a Typhoon Trio imager (GE Healthcare).

Cap addition by lysyl-tRNA synthetase—Triphosphorylated *yeiP* RNA (5 ng) synthesized by *in vitro* transcription was treated with *E. coli* LysU (1 μM) for 4 hr at 37°C in a solution (15 μl) containing Tris-HCl, pH 8.0 (100 mM), $MgCl_2$ (10 mM), $ZnCl_2$ (0.1 mM), ATP (10 mM), lysine (1 mM), inorganic pyrophosphatse (0.1 units), and rRNasin (20 units). The reaction was quenched with EDTA (210 μl of a 3.5 mM solution), and the RNA was recovered by phenol extraction and ethanol precipitation. As a control, a portion of each reaction product was subsequently decapped by treatment with excess RppH (200 nM for 2 hr at 37°C). The *yeiP* RNA was then cleaved site-specifically 69 nt from the 5′ end with a 10-23 deoxyribozyme (DZyeiP69) and analyzed by boronate gel electrophoresis and Northern blotting with a complementary 5′ end-labeled oligonucleotide probe.

mRNA half-life measurements—To examine the contributions of ApaH and RppH to rates of decapping in the absence of stress, isogenic Δ*araE* Δ*araH* Δ*apaH* strains of *E. coli* containing plasmid pPBAD-ApaH30 or pPM30-araE were grown to mid-log phase at 37°C in LB medium and treated for 30 min with L-arabinose (0.2% v/v for *yeiP* and 0.1% v/v for *trxB*) to induce ApaH synthesis in the strain containing plasmid pPBAD-ApaH30 and then with rifampicin (200 μg/ml) to arrest transcription. Total RNA was extracted at time intervals thereafter, and equal amounts (10 μg) were cut with a 10-23 deoxyribozyme (DZyeiP69 or DZtrxB48) specific for *yeiP* or *trxB* mRNA, subjected to electrophoresis on a boronate gel to separate capped from uncapped RNA, and analyzed by Northern blotting. Bands corresponding to capped *yeiP* or *trxB* mRNA were detected with a complementary 5′ end-labeled oligonucleotide probe, visualized on a Typhoon Trio imager (GE Healthcare), and quantified by using ImageQuant TL software. First-order rate constants for the disappearance of capped *yeiP* or *trxB* mRNA were calculated as described below.

To measure the aggregate half-lives of individual mRNAs in the absence of stress, *E. coli* cells were grown to mid-log phase at 37°C in MOPS-glucose medium, and total RNA was extracted at time intervals after inhibiting transcription with rifampicin (200 μg/ml). Equal amounts of each sample (10 μg) were either left untreated (*yeiP* mRNA) or cut with a 10-23 deoxyribozyme (DZtrxB95) specific for *trxB* mRNA. The RNA was then subjected to electrophoresis on an ordinary polyacrylamide gel and analyzed by Northern blotting. Bands

Author Manuscript Author Manuscript Author Manuscript Author Manuscript

corresponding to *yeiP* or *trxB* mRNA were detected with a complementary 5′ end-labeled oligonucleotide probe, and half-lives were calculated as described below.

To measure the half-life of capped mRNAs during disulfide stress, $CdCl_2$ (0.2 mM) was added to cells growing exponentially at 37°C in MOPS-glucose medium, and transcription was arrested 90 min later with rifampicin (200 μg/ml). Total RNA was extracted at time intervals thereafter, and equal amounts (10 μg) were cut with a 10-23 deoxyribozyme (DZyeiP69 or DZtrxB95) specific for *yeiP* or *trxB* mRNA and analyzed by boronate gel electrophoresis and Northern blotting to separate capped from uncapped RNA. Bands corresponding to capped *yeiP* or *trxB* mRNA were detected with a complementary 5′ end-labeled oligonucleotide probe, and half-lives were calculated as described above.

ApaH inactivation by $CdCl_2$ and diamide—Purified ApaH (200 nM) was combined with $CdCl_2$ (0.2 mM), diamide (2 mM), or no inactivating agent in a solution (10 μl) containing HEPES, pH 7.6 (20 mM), $MgCl_2$ (5 mM), and glycerol (1% v/v) and incubated at 37°C. After 60 min, the product was combined with an equal volume of total cellular RNA (5 μg) from *E. coli* Δ*apaH* cells, dissolved in the same buffer, and the mixture was incubated at 37°C for an additional 15 min. The reaction was quenched with EDTA (210 μl of a 3.5 mM solution), and the RNA products were phenol extracted, ethanol precipitated, cut with a 10-23 deoxyribozyme (DZyeiP69) specific for *yeiP* mRNA, and analyzed by boronate gel electrophoresis and Northern blotting with a 5′ end-labeled oligonucleotide probe complementary to *yeiP* mRNA.

QUANTIFICATION AND STATISTICAL ANALYSIS

Quantification of band intensities—Band intensities were quantified by using ImageQuant TL software. They were normalized either to one another (two bands in the same gel lane) when calculating the fraction of a particular transcript that was capped or ligated or to total RNA loaded in the gel lane when measuring degradation rates by Northern blotting.

Calculation of capped RNA percentages, reaction yields, rate constants, and half-lives—Tables 1, S1, S3, and S5 list mean values and standard deviations of three biological replicates (Tables 1 and S5) or three technical replicates (Tables S1 and S3). First-order rate constants (k) and half-lives ($t_{½}$) for RNA degradation were calculated from the slope of the best-fit line for the data graphed semilogarithmically in Figures 5, 6, and S2, as determined by linear regression (k = –slope; $t_{½} = \ln 2 / k$), and standard deviations were calculated from the standard deviation of each slope. The rate constant for RppH-mediated decapping in *E. coli* was calculated by substracting the rate constant for the disappearance of the capped transcript in Δ*apaH* ΔrppH cells from the corresponding rate constant in Δ*apaH* cells. The rate constant for ApaH-mediated decapping in *E. coli* was calculated by substracting the rate constant for the disappearance of the capped transcript in Δ*apaH* cells from the corresponding rate constant when ApaH synthesis from an ectopic P_{BAD}-*apaH* gene was induced with arabinose.

Author Manuscript Author Manuscript Author Manuscript Author Manuscript

Statistical extrapolation—The likelihood that a given percentage or more of all *E. coli* transcripts are Np_4-capped to some extent in cadmium-stressed cells was calculated by solving the following equation for the value of r:

$$\int_0^m p^x(1-p)^{n-x}\mathrm{d}p = \frac{x!(n-x)!(1-r)}{(n+1)!}$$

where p is the probability that a randomly selected *E. coli* transcript is capped to some extent ($0 \le p \le 1$), n is the number of transcripts tested, x is the number of tested transcripts found to be capped to some extent, m is the minimum fraction of all *E. coli* transcripts postulated to be capped to some extent, and r is the likelihood that the true value of p is greater than m (Hansen et al., 1994). Since all 15 examined transcripts were capped to some extent in cadmium-stressed cells ($n = 15$ and $x = 15$), one can calculate from this equation that there is an 81% probability (r) that more than 90% (m) of all *E. coli* transcripts are capped to some extent under those conditions.

esCAPade calculations—The PABLO ligation efficiencies of the monophosphorylated and diphosphorylated *yeiP* standards (E_{LM} and E_{LD}, respectively; $E_{LT} = 0$) were calculated as follows:

$$E_{LM} = \frac{Y_{LM}}{M_S}$$
$$E_{LD} = \frac{Y_{LD}}{D_S}$$

where Y_{LM} and Y_{LD} were the fractional PABLO ligation yields measured for the monophosphorylated and diphosphorylated standards, respectively, and M_S and D_S were the fraction of those standards that were monophosphorylated or diphosphorylated, as estimated from the molar ratio of NMP or NDP to the corresponding NTP during their synthesis by *in vitro* transcription (Luciano et al., 2017; Luciano and Belasco, 2019).

The PACO capping efficiencies of the monophosphorylated, diphosphorylated, and triphosphorylated *yeiP* standards synthesized by *in vitro* transcription (E_{CM}, E_{CD}, and E_{CT}, respectively) were calculated as follows:

$$E_{CM} = \frac{Y_{CM} - Y_{CT}(1 - M_S)}{M_S}$$
$$E_{CD} = \frac{Y_{CD} - Y_{CT}(1 - D_S)}{D_S}$$
$$E_{CT} = Y_{CT}$$

where Y_{CM}, Y_{CD}, and Y_{CT} were the fractional PACO capping yields measured for the monophosphorylated, diphosphorylated, and triphosphorylated standards, respectively, and

Author Manuscript Author Manuscript Author Manuscript Author Manuscript

M_S and D_S were the fraction of those standards that were monophosphorylated or diphosphorylated (Luciano et al., 2017; Luciano and Belasco, 2019).

The fraction of the Ap_3-, Ap_4-, and Ap_5-capped *yeiP* standards that actually bore a cap (P_3, P_4, and P_5, respectively) was determined by boronate gel electrophoresis and Northern blotting, and the fraction of each that was monophosphorylated or diphosphorylated after phosphatase treatment and decapping by ApaH (M_3, D_3, M_4, D_4, M_5, and D_5, respectively) was ascertained by PABLO and PAcO as follows:

$$M = \frac{Y_L - E_{LD}(D)}{E_{LM}}$$

$$D = \frac{Y_C - E_{CT}(1 - M) - E_{CM}(M)}{E_{CD} - E_{CT}}$$

where M is the fraction of monophosphorylated 5′ ends after decapping, D is the fraction of diphosphorylated 5′ ends after decapping, Y_L is the measured PABLO ligation yield, Y_C is the measured PACO capping yield, E_{LM} and E_{LD} are the measured ligation efficiencies of the monophosphorylated and diphosphorylated standards, respectively, and E_{CM}, E_{CD}, and E_{CT} are the measured capping efficiencies of the monophosphorylated, diphosphorylated, and triphosphorylated standards, respectively. The interdependence of the calculations of D and M made it necessary to calculate these values iteratively until each achieved convergence (Luciano et al., 2017; Luciano and Belasco, 2019). The fractional yield of monophosphorylated and diphosphorylated products obtained by decapping the Ap_3-, Ap_4-, and Ap_5-capped standards (M_3/P_3, D_3/P_3, M_4/P_4, D_4/P_4, M_5/P_5, and D_5/P_5, respectively) was then calculated from the ratio of these values. The fractional yield of decapped products that were triphosphorylated was calculated by subtraction ($T_n/P_n = 1 - D_n/P_n - M_n/P_n$).

Parallel measurements and calculations were performed on *yeiP* mRNA from wild-type *E. coli* cells experiencing cadmium stress and from unstressed *E. coli* Δ*apaH* cells to determine the fraction that was capped (C), the fractional yield of monophosphorylated, diphosphorylated, and triphosphorylated products obtained after phosphatase treatment and decapping by ApaH (M_C, D_C, and T_C, respectively), and the corresponding ratios (M_C/C, D_C/C, and T_C/C, respectively). By comparing these values to those for the *in vitro* transcribed standards, we were able to calculate the fraction of *yeiP* mRNA in *E. coli* that bears an Np_3, Np_4, or Np_5 cap (P_{3C}, P_{4C}, and P_{5C}, respectively) by applying Cramer's rule to the following set of linear equations:

$$M_C = (M_3 / P_3)P_{3C} + (M_4 / P_4)P_{4C} + (M_5 / P_5)P_{5C}$$

$$D_C = (D_3 / P_3)P_{3C} + (D_4 / P_4)P_{4C} + (D_5 / P_5)P_{5C}$$

$$C = P_{3C} + P_{4C} + P_{5C}$$

Finally, the fraction of *yeiP* caps containing three, four, or five bridging phosphates was calculated by normalizing these values to the overall fraction of *yeiP* mRNA that was capped (P_{3C}/C, P_{4C}/C, and P_{5C}/C, respectively).

Author Manuscript Author Manuscript Author Manuscript Author Manuscript

In this manner, the number of phosphates in an RNA cap could be determined by direct calculation. However, the complexity of the equations made it difficult to calculate the standard deviations of P_{3C}, P_{4C}, P_{5C}, and the other parameters directly from the mean values and standard deviations of the original measurements. These errors could nevertheless be determined by Monte Carlo simulation, as follows. The mean values and standard deviations of the measurements (Tables S1, S3, and S5) were first used to generate random Gaussian sample sets of 100,000 values for each of the variables, which were then used to calculate the parameter of interest. For each simulation, a histogram was constructed and fit to a spline function, and the mode (peak value) was determined. Because of the asymmetry of the distribution, an asymmetrical error equivalent to one standard deviation was then calculated by integrating outward from the mode until a confidence level of 68.3% was attained. These modes and errors are reported in Tables S2, S4, and S6.

Supplementary Material

Refer to Web version on PubMed Central for supplementary material.

ACKNOWLEDGMENTS

We are grateful to Venu Kamarthapu for purified *E. coli* RNA polymerase, Tricia Foley for purified T4 DNA ligase, and Vitaly Epshtein, Kevin Belasco, Monika Raj, Jamie Richards, and Monica Hui for help and advice. This research was supported by fellowships to D.J.L. and R.L.-P. from the National Institutes of Health (T32AI007180 and T32GM007308), a fellowship to D.J.L. from the Vilcek endowment, and research grants to J.G.B. (R01GM035769 and R01GM112940) from the National Institutes of Health.

REFERENCES

Antelmann H, and Helmann JD (2011). Thiol-based redox switches and gene regulation. Antioxid. Redox Signal 14, 1049–1063. [PubMed: 20626317]

Åslund F, and Beckwith J (1999). Bridge over troubled waters: sensing stress by disulfide bond formation. Cell 96, 751–753. [PubMed: 10102262]

Baba T, Ara T, Hasegawa M, Takai Y, Okumura Y, Baba M, Datsenko KA, Tomita M, Wanner BL, and Mori H (2006). Construction of *Escherichia coli* K-12 in-frame, single-gene knockout mutants: the Keio collection. Mol. Syst. Biol 2, 2006.0008.

Beavers WN, and Skaar EP (2016). Neutrophil-generated oxidative stress and protein damage in Staphylococcus aureus. Pathog. Dis 74, ftw060. [PubMed: 27354296]

Bessman MJ, Walsh JD, Dunn CA, Swaminathan J, Weldon JE, and Shen J (2001). The gene *ygdP*, associated with the invasiveness of *Escherichia coli* K1, designates a Nudix hydrolase, Orf176, active on adenosine (5')-pentaphospho-(5')-adenosine (Ap5A). J. Biol. Chem 276, 37834–37838. [PubMed: 11479323]

Bird JG, Zhang Y, Tian Y, Panova N, Barvik I, Greene L, Liu M, Buckley B, Krásny L, Lee JK, et al. (2016). The mechanism of RNA 5' capping with NAD+, NADH and desphospho-CoA. Nature 535, 444–447. [PubMed: 27383794]

Bochner BR, Lee PC, Wilson SW, Cutler CW, and Ames BN (1984). AppppA and related adenylylated nucleotides are synthesized as a consequence of oxidation stress. Cell 37, 225–232. [PubMed: 6373012]

Boulos S, Razin E, Nechushtan H, and Rachmin I (2016). Diadenosine tetraphosphate (Ap4A) in health and disease In Modified Nucleic Acids in Biology and Medicine, Jurga S, Erdmann VA, and Barciszewski J, eds. (Switzerland: Springer), pp. 207–219.

Brevet A, Chen J, Lévêque F, Plateau P, and Blanquet S (1989). In vivo synthesis of adenylylated bis(5'-nucleosidyl) tetraphosphates (Ap4N) by *Escherichia coli* aminoacyl-tRNA synthetases. Proc. Natl. Acad. Sci. USA 86, 8275–8279. [PubMed: 2554306]

Author Manuscript Author Manuscript Author Manuscript Author Manuscript

Cahová H, Winz ML, Höfer K, Nübel G, and Jäschke A (2015). NAD captureSeq indicates NAD as a bacterial cap for a subset of regulatory RNAs. Nature 519, 374–377. [PubMed: 25533955]

Cartwright JL, Britton P, Minnick MF, and McLennan AG (1999). The *IalA* invasion gene of *Bartonella bacilliformis* encodes a (di)nucleoside polyphosphate hydrolase of the MutT motif family and has homologs in other invasive bacteria. Biochem. Biophys. Res. Commun 256, 474–479. [PubMed: 10080922]

Celesnik H, Deana A, and Belasco JG (2007). Initiation of RNA decay in *Escherichia coli* by 5' pyrophosphate removal. Mol. Cell 27, 79–90. [PubMed: 17612492]

Coste H, Brevet A, Plateau P, and Blanquet S (1987). Non-adenylylated bis(5'-nucleosidyl) tetraphosphates occur in *Saccharomyces cerevisiae* and in *Escherichia coli* and accumulate upon temperature shift or exposure to cadmium. J. Biol. Chem 262, 12096–12103. [PubMed: 3305502]

Datsenko KA, and Wanner BL (2000). One-step inactivation of chromosomal genes in *Escherichia coli* K-12 using PCR products. Proc. Natl. Acad. Sci. USA 97, 6640–6645. [PubMed: 10829079]

Deana A, Celesnik H, and Belasco JG (2008). The bacterial enzyme RppH triggers messenger RNA degradation by 5' pyrophosphate removal. Nature 451, 355–358. [PubMed: 18202662]

Delalande O, Desvaux H, Godat E, Valleix A, Junot C, Labarre J, and Boulard Y (2010). Cadmium-glutathione solution structures provide new insights into heavy metal detoxification. FEBS J. 277, 5086–5096. [PubMed: 21078121]

Doamekpor SK, Sanchez AM, Schwer B, Shuman S, and Lima CD (2014). How an mRNA capping enzyme reads distinct RNA polymerase II and Spt5 CTD phosphorylation codes. Genes Dev. 28, 1323–1336. [PubMed: 24939935]

Farr SB, Arnosti DN, Chamberlin MJ, and Ames BN (1989). An *apaH* mutation causes AppppA to accumulate and affects motility and catabolite repression in *Escherichia coli*. Proc. Natl. Acad. Sci. USA 86, 5010–5014. [PubMed: 2544886]

Finamore FJ, and Warner AH (1963). The occurrence of P1, P4-diguanosine 5'-tetraphosphate in brine shrimp eggs. J. Biol. Chem 238, 344–348. [PubMed: 13945193]

Foley PL, Hsieh PK, Luciano DJ, and Belasco JG (2015). Specificity and evolutionary conservation of the *Escherichia coli* RNA pyrophosphohydrolase RppH. J. Biol. Chem 290, 9478–9486. [PubMed: 25657006]

Fraga H, and Fontes R (2011). Enzymatic synthesis of mono and dinucleoside polyphosphates. Biochim. Biophys. Acta 1810, 1195–1204. [PubMed: 21978831]

Guranowski A, Jakubowski H, and Holler E (1983). Catabolism of diadenosine 5',5'"-P1,P4-tetraphosphate in procaryotes. Purification and properties of diadenosine 5',5'"-P1,P4-tetraphosphate (symmetrical) pyrophosphohydrolase from *Escherichia coli* K12. J. Biol. Chem 258, 14784–14789. [PubMed: 6317672]

Hansen MJ, Chen L-H, Fejzo MLS, and Belasco JG (1994). The *ompA* 5' untranslated region impedes a major pathway for mRNA degradation in *Escherichia coli*. Mol. Microbiol 12, 707–716. [PubMed: 8052123]

Hansen S, Lewis K, and Vulic M (2008). Role of global regulators and nucleotide metabolism in antibiotic tolerance in *Escherichia coli*. Antimicrob. Agents Chemother 52, 2718–2726. [PubMed: 18519731]

Helbig K, Grosse C, and Nies DH (2008). Cadmium toxicity in glutathione mutants of *Escherichia coli*. J. Bacteriol 190, 5439–5454. [PubMed: 18539742]

Hossain ST, Mallick I, and Mukherjee SK (2012). Cadmium toxicity in *Escherichia coli*: Cell morphology, Z-ring formation and intracellular oxidative balance. Ecotoxicol. Environ. Saf 86, 54–59. [PubMed: 23063080]

Igloi GL, and Kössel H (1985). Affinity electrophoresis for monitoring terminal phosphorylation and the presence of queuosine in RNA. Application of polyacrylamide containing a covalently bound boronic acid. Nucleic Acids Res. 13, 6881–6898. [PubMed: 2414733]

Ismail TM, Hart CA, and McLennan AG (2003). Regulation of dinucleoside polyphosphate pools by the YgdP and ApaH hydrolases is essential for the ability of *Salmonella enterica* serovar typhimurium to invade cultured mammalian cells. J. Biol. Chem 278, 32602–32607. [PubMed: 12824172]

Author Manuscript Author Manuscript Author Manuscript Author Manuscript

Itaya M, Omori A, Kanaya S, Crouch RJ, Tanaka T, and Kondo K (1999). Isolation of RNase H genes that are essential for growth of *Bacillus subtilis* 168. Journal of bacteriology 181, 2118–2123. [PubMed: 10094689]

Ivanov AE, Larsson H, Galaev IY, and Mattiasson B (2004). Synthesis of boronate-containing copolymers of N,N-dimethylacrylamide, their interaction with poly(vinyl alcohol) and rheological behaviour of the gels. Polymer 45, 2495–2505.

Ji X, Zou J, Peng H, Stolle AS, Xie R, Zhang H, Peng B, Mekalanos JJ, and Zheng J (2019). Alarmone Ap4A is elevated by aminoglycoside antibiotics and enhances their bactericidal activity. Proc. Natl. Acad. Sci. USA 116, 9578–9585. [PubMed: 31004054]

Johnstone DB, and Farr SB (1991). AppppA binds to several proteins in *Escherichia coli*, including the heat shock and oxidative stress proteins DnaK, GroEL, E89, C45 and C40. EMBO J. 10, 3897–3904. [PubMed: 1935909]

Kim D, Hong JS, Qiu Y, Nagarajan H, Seo JH, Cho BK, Tsai SF, and Palsson BØ (2012). Comparative analysis of regulatory elements between *Escherichia coli* and *Klebsiella pneumoniae* by genome-wide transcription start site profiling. PLoS Genet. 8, e1002867. [PubMed: 22912590]

Kisselev LL, Justesen I, Wolfson AD, and Frolova LY (1998). Diadenosine oligophosphates (Ap(n)A), a novel class of signalling molecules? FEBS Lett. 427, 157–163. [PubMed: 9607303]

Kosower NS, and Kosower EM (1995). Diamide: an oxidant probe for thiols. Methods Enzymol. 257, 123–133.

Lee PC, Bochner BR, and Ames BN (1983). AppppA, heat-shock stress, and cell oxidation. Proc. Natl. Acad. Sci. USA 80, 7496–7500. [PubMed: 6369319]

Lee YN, Nechushtan H, Figov N, and Razin E (2004). The function of lysyl-tRNA synthetase and Ap4A as signaling regulators of MITF activity in FcεRI-activated mast cells. Immunity 20, 145–151. [PubMed: 14975237]

Leichert LIO, Scharf C, and Hecker M (2003). Global characterization of disulfide stress in *Bacillus subtilis*. J. Bacteriol 185, 1967–1975. [PubMed: 12618461]

Lévêque F, Blanchin-Roland S, Fayat G, Plateau P, and Blanquet S (1990). Design and characterization of *Escherichia coli* mutants devoid of Ap4N-hydrolase activity. J. Mol. Biol 212, 319–329. [PubMed: 2157025]

Luciano DJ, and Belasco JG (2019). Analysis of RNA 5' ends: Phosphate enumeration and cap characterization. Methods 155, 3–9. [PubMed: 30419334]

Luciano DJ, Vasilyev N, Richards J, Serganov A, and Belasco JG (2017). A novel RNA phosphorylation state enables 5′ end-dependent degradation in *Escherichia coli*. Mol. Cell 67, 44–54. [PubMed: 28673541]

Mackie GA (1998). Ribonuclease E is a 5'-end-dependent endonuclease. Nature 395, 720–723. [PubMed: 9790196]

Meacock PA, and Cohen SN (1980). Partitioning of bacterial plasmids during cell division: a cis-acting locus that accomplishes stable plasmid inheritance. Cell 20, 529–542. [PubMed: 6248248]

Monds RD, Newell PD, Wagner JC, Schwartzman JA, Lu W, Rabinowitz JD, and O'Toole GA (2010). Di-adenosine tetraphosphate (Ap4A) metabolism impacts biofilm formation by *Pseudomonas fluorescens* via modulation of c-di-GMP-dependent pathways. J. Bacteriol 192, 3011–3023. [PubMed: 20154123]

Müller A, Hoffmann JH, Meyer HE, Narberhaus F, Jakob U, and Leichert LI (2013). Nonnative disulfide bond formation activates the σ32-dependent heat shock response in *Escherichia coli*. J. Bacteriol 195, 2807–2816. [PubMed: 23585533]

Neidhardt FC, Bloch PL, and Smith DF (1974). Culture medium for enterobacteria. J. Bacteriol 119, 736–747. [PubMed: 4604283]

Nishimura A, Moriya S, Ukai H, Nagai K, Wachi M, and Yamada Y (1997). Diadenosine 5',5'"-P1,P4-tetraphosphate (Ap4A) controls the timing of cell division in *Escherichia coli*. Genes Cells 2, 401–413. [PubMed: 9286857]

Nudler E, Gusarov I, and Bar-Nahum G (2003). Methods of walking with the RNA polymerase. Methods Enzymol 371, 160–169. [PubMed: 14712698]

Plateau P, and Blanquet S (1994). Dinucleoside oligophosphates in micro-organisms. Adv. Microb. Physiol 36, 81–109. [PubMed: 7942317]

Author Manuscript Author Manuscript Author Manuscript Author Manuscript

Plateau P, Fromant M, Brevet A, Gesquière A, and Blanquet S (1985). Catabolism of bis(5'-nucleosidyl) oligophosphates in *Escherichia coli*: metal requirements and substrate specificity of homogeneous diadenosine-5',5'''-P1,P4-tetraphosphate pyrophosphohydrolase. Biochemistry 24, 914–922. [PubMed: 2986688]

Plateau P, Fromant M, Kepes F, and Blanquet S (1987). Intracellular 5',5'-dinucleoside polyphosphate levels remain constant during the *Escherichia coli* cell cycle. J. Bacteriol 169, 419–422. [PubMed: 3539924]

Randerath K, Janeway CM, Stephenson ML, and Zamecnik PC (1966). Isolation and characterization of dinucleoside tetra- and tri-phosphates formed in the presence of lysyl-sRNA synthetase. Biochem. Biophys. Res. Commun 24, 98–105. [PubMed: 4290754]

Richards J, Luciano DJ, and Belasco JG (2012). Influence of translation on RppH-dependent mRNA degradation in *Escherichia coli*. Mol. Microbiol 86, 1063–1072. [PubMed: 22989003]

Santoro SW, and Joyce GF (1997). A general purpose RNA-cleaving DNA enzyme. Proc. Natl. Acad. Sci. USA 94, 4262–4266. [PubMed: 9113977]

Song MG, Bail S, and Kiledjian M (2013). Multiple Nudix family proteins possess mRNA decapping activity. RNA 19, 390–399. [PubMed: 23353937]

Varshavsky A (1983). Diadenosine 5', 5'''-P1, P4-tetraphosphate: a pleiotropically acting alarmone? Cell 34, 711–712. [PubMed: 6354469]

Vvedenskaya IO, Bird JG, Zhang Y, Zhang Y, Jiao X, Barvik I, Krásný L, Kiledjian M, Taylor DM, Ebright RH, et al. (2018). CapZyme-Seq Comprehensively Defines Promoter-Sequence Determinants for RNA 5' Capping with NAD+. Mol. Cell 70, 553–564. [PubMed: 29681497]

Zamecnik PC, Stephenson ML, Janeway CM, and Randerath K (1966). Enzymatic synthesis of diadenosine tetraphosphate and diadenosine triphosphate with a purified lysyl-sRNA synthetase. Biochem. Biophys. Res. Commun 24, 91–97. [PubMed: 5338216]

Zheng M, Aslund F, and Storz G (1998). Activation of the OxyR transcription factor by reversible disulfide bond formation. Science 279, 1718–1721. [PubMed: 9497290]

Author Manuscript Author Manuscript Author Manuscript Author Manuscript

Highlights

- Disulfide stress induces widespread Np_4 capping of RNA transcripts in *E. coli*
- *In vitro*, Np_4 caps can be added by RNA polymerase or aminoacyl-tRNA synthetases
- Np_4 caps are removed in *E. coli* by ApaH and RppH, triggering rapid RNA degradation
- ApaH acts as both a sensor and an effector of disulfide stress, which inactivates it

Author Manuscript Author Manuscript Author Manuscript Author Manuscript

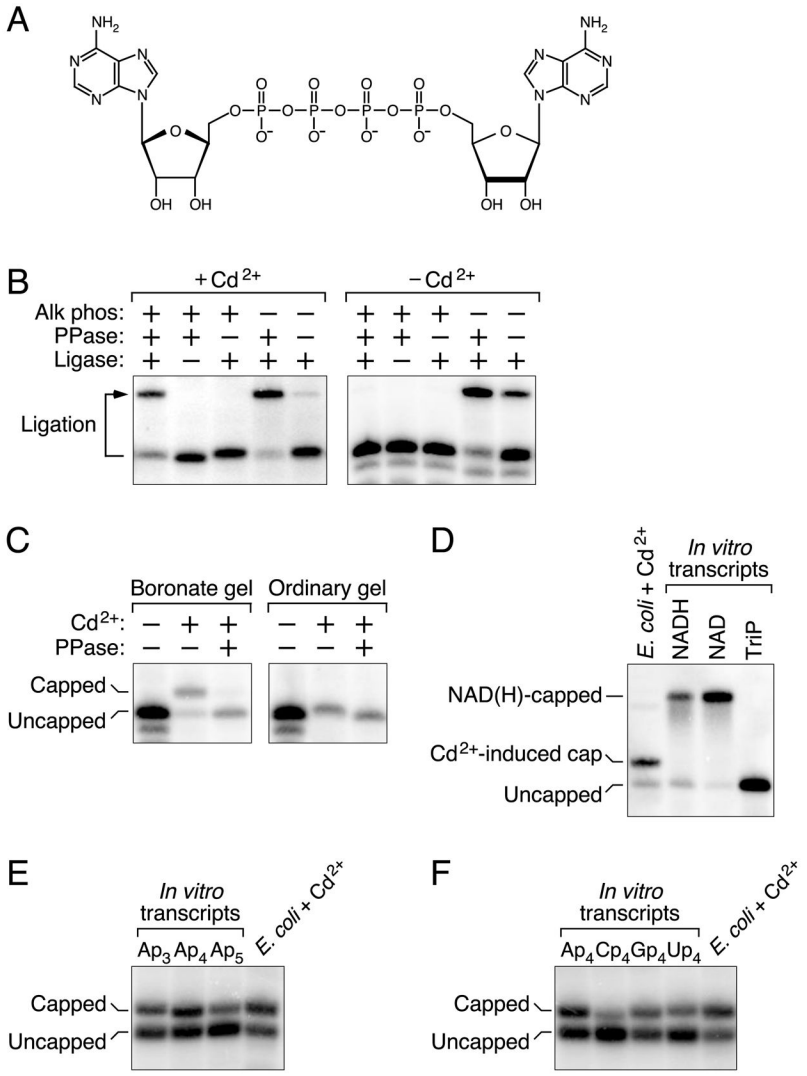

Figure 1. Detection of capped RNA in *E. coli* cells treated with cadmium chloride.

(A) Structure of the dinucleoside tetraphosphate AP_4A.

(B) Protection of the 5′ phosphates of *yeiP* mRNA. Total RNA from *E. coli* cells that had or had not been treated with cadmium chloride was treated sequentially with alkaline phosphatase (Alk phos) and tobacco acid pyrophosphatase (PPase), and any monophosphorylated *yeiP* transcripts that resulted were detected by the ability of their 5′ termini to undergo splinted ligation to a DNA oligonucleotide (Ligase). The bent arrow leads from the full-length *yeiP* transcript to its ligation product. RNAs migrating more rapidly than the full-length transcript correspond to degradation intermediates of *yeiP* mRNA in *E. coli*; these would not have undergone splinted ligation regardless of their 5′ phosphorylation state. See also Fig. S1A.

(C) Detection of capped *yeiP* mRNA by boronate gel electrophoresis. Total RNA from *E. coli* cells that had or had not been treated with cadmium chloride was cleaved site-specifically 69 nt from the *yeiP* 5′ end with a 10-23 deoxyribozyme (Santoro and Joyce, 1997) so as to generate a 5′-terminal fragment bearing a 2′,3′ cyclic phosphate rather than a vicinal diol at its 3′ end. The RNA was then subjected to electrophoresis on a boronate gel

Author Manuscript Author Manuscript Author Manuscript Author Manuscript

or an ordinary polyacrylamide gel, with or without prior decapping (PPase), and *yeiP* RNA was detected by Northern blotting (Luciano and Belasco, 2019).

(D) Distinct electrophoretic mobility on a boronate gel of capped *yeiP* mRNA from cadmium-treated cells and NAD- or NADH-capped *yeiP* standards synthesized *in vitro*. TriP, triphosphorylated *yeiP* standard.

(E) Similar electrophoretic mobility on a boronate gel of capped *yeiP* mRNA from cadmium-treated cells and Ap_3-, Ap_4-, and Ap_5-capped *yeiP* standards synthesized *in vitro*.

(F) Similar electrophoretic mobility on a boronate gel of capped *yeiP* mRNA from cadmium-treated cells and Ap_4-, Cp_4-, Gp_4-, and Up_4-capped *yeiP* standards synthesized *in vitro*.

Author Manuscript Author Manuscript Author Manuscript Author Manuscript

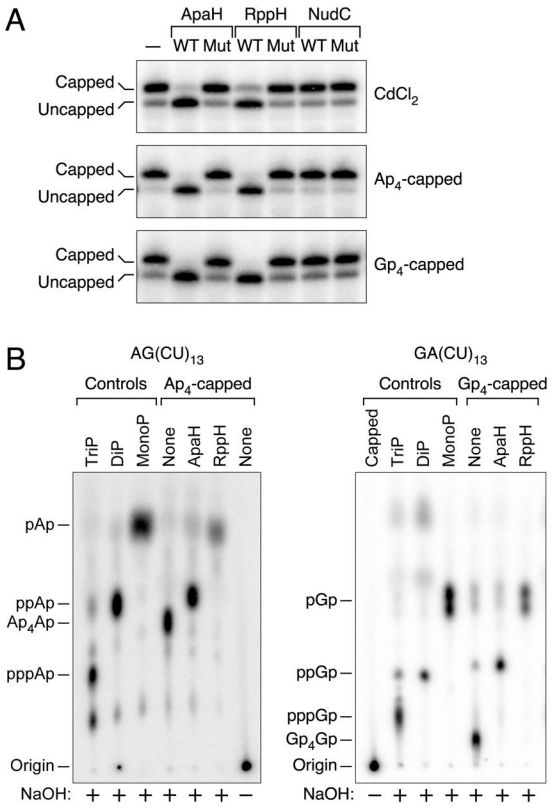

Figure 2. Decapping enzymes and their reaction products.

(A) Decapping *in vitro*. Purified ApaH, RppH, and NudC and catalytically inactive mutants thereof were each tested for their ability to decap *yeiP* mRNA that had been extracted from cadmium-treated cells ($CdCl_2$) or had been synthesized with a 5′-terminal Ap_4 or Gp_4 cap by *in vitro* transcription. Decapping was detected by boronate gel electrophoresis and blotting. WT, wild-type enzyme; Mut, mutant enzyme lacking catalytic activity; –, no enzyme. See also Figs. S2A, S3, and S7C.

(B) Phosphorylation state of the RNA product of decapping by ApaH or RppH. Ap_4-capped $AG(CU)_{13}$ (left) and Gp_4-capped $GA(CU)_{13}$ (right) bearing a single ^{32}P label between the first and second nucleotides were treated with purified ApaH or RppH. The radiolabeled products were subjected to alkaline hydrolysis (NaOH) and then analyzed by thin layer chromatography. Control markers were generated by hydrolyzing triphosphorylated (TriP), diphosphorylated (DiP), or monophosphorylated (MonoP) $AG(CU)_{13}$ and $GA(CU)_{13}$ without prior enzyme treatment.

Author Manuscript Author Manuscript Author Manuscript Author Manuscript

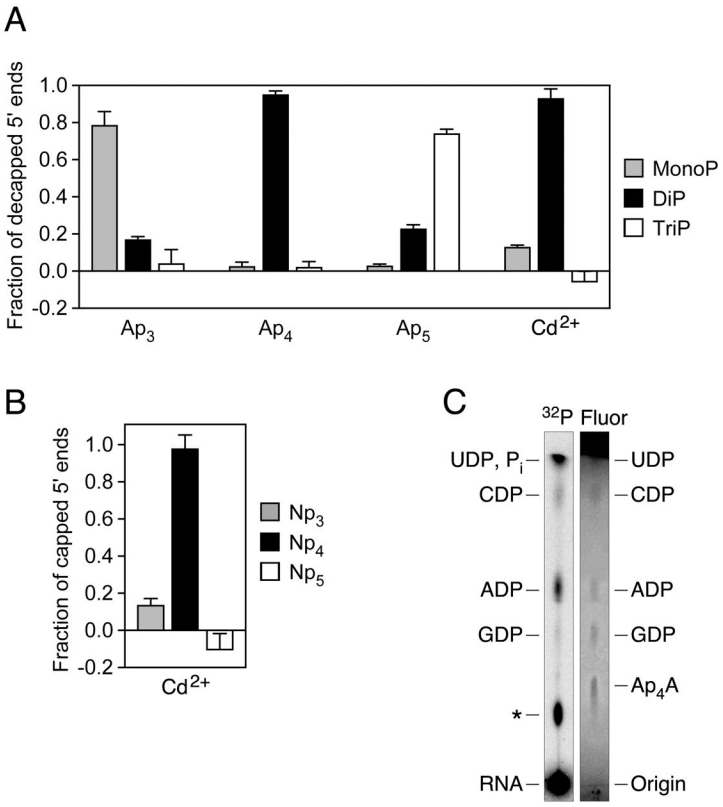

Figure 3. Phosphate content and nucleobase of caps.

(A) Phosphorylation state of the products of *yeiP* decapping by ApaH. *In vitro* transcribed *yeiP* RNA bearing an Ap_3, Ap_4, or Ap_5 cap or *yeiP* RNA extracted from cadmium-treated *E. coli* cells (Cd^{2+}) was treated with alkaline phosphatase and then with ApaH, and the fraction of the decapped *yeiP* 5′ ends that were monophosphorylated (MonoP) or diphosphorylated (DiP) was determined by PABLO or PACO, respectively (Celesnik et al., 2007; Luciano et al., 2017; Luciano and Belasco, 2019). The remainder was assumed to be triphosphorylated (TriP). Each of the synthetic *yeiP* standards was spiked into total RNA from *E. coli* Δ*yeiP* cells to simulate the reaction of a complex mixture of cellular RNAs. Each value was calculated by using data from three experimental replicates (technical replicates for the capped standards and biological replicates for the cellular RNA). Error bars correspond to a confidence level of 68.3%, equivalent to one standard deviation. See also Figs. S1, S4 and S7A and Tables S1-S6.

(B) Calculated fraction of capped *yeiP* 5′ ends bearing an Np_3, Np_4, or Np_5 cap in cells treated with cadmium chloride, as determined by esCAPade. The data from panel A were used to calculate each value. Error bars correspond to a confidence level of 68.3%. See also Table S6

(C) Characterization of the cap nucleobase. Total RNA extracted from *E. coli* cells that had been radiolabeled with [^{32}P] phosphate and exposed to cadmium chloride was treated with alkaline phosphatase to convert uncapped 5′ ends to hydroxyls and hydrolyze any contaminating mononucleotides. It was then fractionated by sucrose-gradient centrifugation, and RNAs 100-1,400 nt long were further separated from nucleotide contaminants by size-exclusion chromatography on Sephadex G-25. The RNA was subsequently treated with

Author Manuscript Author Manuscript Author Manuscript Author Manuscript

ApaH, and the radiolabeled nucleotides thereby released were purified by another round of size-exclusion chromatography, mixed with a set of unlabeled nucleotide standards, and analyzed by thin-layer chromatography on fluorescent polyethylenimine-cellulose plates. ^{32}P, radioactivity; Fluor, fluorescence quenched by the nucleotide standards; ✻, unidentified nucleotide; Pi, inorganic phosphate. See also Figs. S5 and S7B.

Author Manuscript Author Manuscript Author Manuscript Author Manuscript

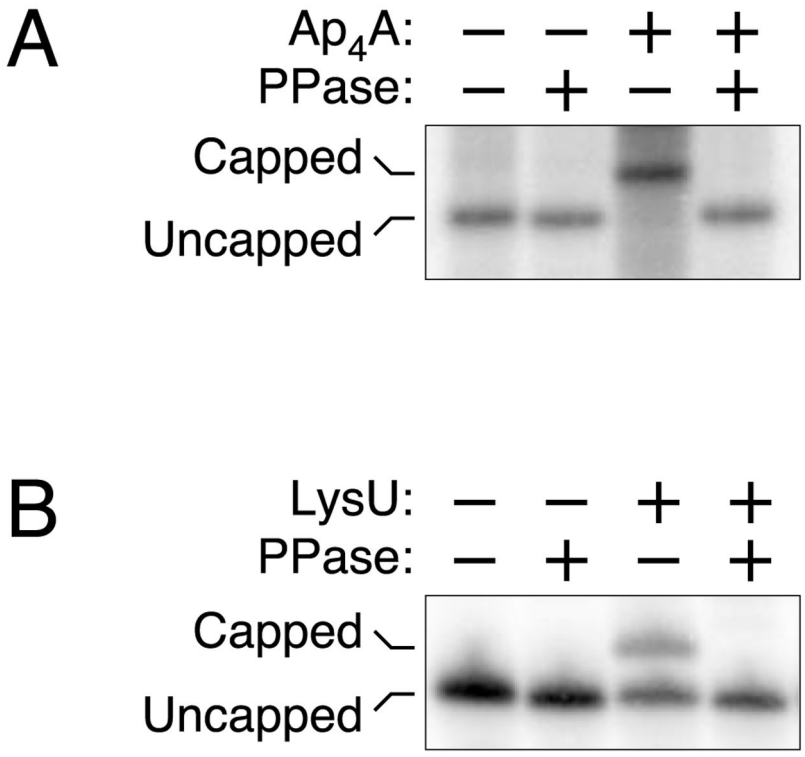

Figure 4. Addition of Np_4 caps.

(A) Incorporation of AP_4A during transcription initiation. *E. coli* RNA polymerase was used to synthesize *yeiP* RNA by *in vitro* transcription in the presence or absence of a substantial excess of Ap_4A, and the products were examined by boronate gel electrophoresis, with or without prior decapping by RppH (PPase). See also Fig. S6A.

(B) Post-transcriptional capping by lysyl-tRNA synthetase. Triphosphorylated *yeiP* RNA was treated with purified *E. coli* LysU in the presence of ATP and lysine, and the reaction products were examined by boronate gel electrophoresis, with or without prior decapping by RppH (PPase). See also Fig. S6B.

Author Manuscript Author Manuscript Author Manuscript Author Manuscript

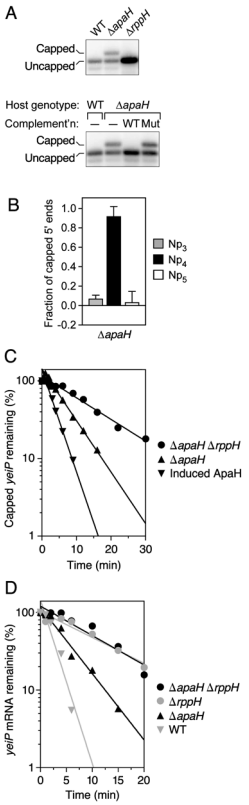

Figure 5. Importance of ApaH and RppH for RNA decapping and degradation in *E. coli*.

(A) Detection of capped *yeiP* mRNA in cells that lack ApaH but not in cells that lack RppH. Total RNA was extracted from unstressed cultures of isogenic wild-type, Δ*apaH*, or Δ*rppH* cells (top) or from Δ*apaH* cells complemented with a plasmid encoding wild-type or catalytically inactive ApaH (bottom), and the presence of capped *yeiP* mRNA was examined by boronate gel electrophoresis and blotting. WT, wild-type *apaH* allele; Mut, mutant *apaH* allele encoding a catalytically inactive enzyme; –, no plasmid. See also Fig. S2B.

(B) Calculated fraction of capped *yeiP* 5′ ends bearing an Np_3, Np_4, or Np_5 cap in Δ*apaH* cells, as determined by esCAPade. The data from Fig. S7A and two additional biological replicates were used to calculate each value (Table S6). Error bars correspond to a confidence level of 68.3%. See also Figs. S1 and S7A and Tables S1-S6.

(C) Rate of loss of capped *yeiP* mRNA after arresting transcription in *E. coli apaH* and *rppH* mutants. Cultures of the indicated strains growing without stress in LB were treated with rifampicin to arrest transcription, and equal amounts of total RNA extracted at time intervals thereafter were analyzed by boronate gel electrophoresis and blotting. Data from representative experiments are shown. See also Fig. S2C.

(D) Effect of an *apaH* deletion on the aggregate decay rate of *yeiP* mRNA in the presence or absence of RppH. Cultures of the indicated strains growing without stress in MOPS-glucose were treated with rifampicin, and equal amounts of total RNA extracted at time intervals thereafter were analyzed by electrophoresis on ordinary polyacrylamide gels. Data from representative experiments are shown. See also Fig. S2D.

Author Manuscript Author Manuscript Author Manuscript Author Manuscript

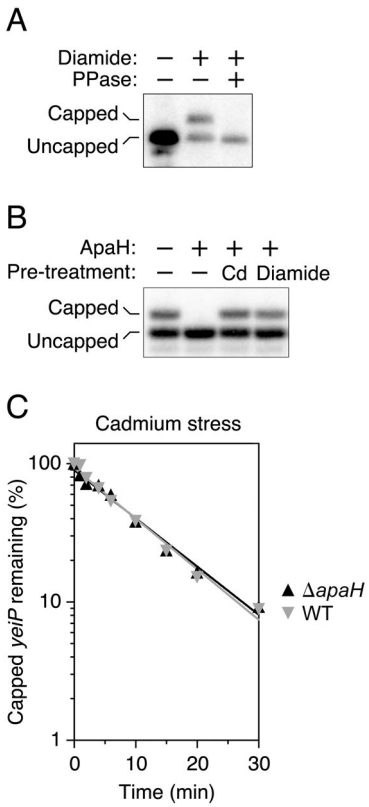

Figure 6. Effect of disulfide stress on RNA capping and degradation in *E. coli*.

(A) Presence of capped *yeiP* mRNA in diamide-treated cells. Total RNA from *E. coli* cells that had or had not been treated with diamide was analyzed by boronate gel electrophoresis and Northern blotting, with or without prior decapping with RppH (PPase). See also Fig. S2E.

(B) Inactivation of ApaH by cadmium and diamide. Purified ApaH was treated with cadmium chloride or diamide, and the decapping activity that remained was analyzed by boronate gel electrophoresis and blotting, using *yeiP* mRNA from a Δ*apaH* strain of *E. coli* as a substrate.

(C) Slow decapping of *yeiP* mRNA in cells experiencing disulfide stress. The indicated strains of *E. coli* growing in MOPS-glucose were treated first with cadmium chloride and then with rifampicin, and equal amounts of total RNA extracted at time intervals thereafter were analyzed by boronate gel electrophoresis and blotting. Data from representative experiments are shown. See also Fig. S2F.

Author Manuscript Author Manuscript Author Manuscript Author Manuscript

Table 1.

Abundance and 5′-terminal transcribed nucleotide of Np_n-capped transcripts.

Transcript	5′-terminal transcribed nucleotide	Cadmium stress (%)	Δ*apaH* (%)
yeiP	A *	76 ± 1	36 ± 1
yeiP-A1G	G *	5 ± 1	9 ± 1
trxB	A	41 ± 1	19 ± 1
rpsT P1	A *	61 ± 1	23 ± 1
rpsT P2	C *	36 ± 1	19 ± 1
ppa	A	43 ± 1	11 ± 1
efp	C *	72 ± 1	25 ± 1
yfcZ	A	60 ± 1	16 ± 1
slyB P1	A	52 ± 2	15 ± 1
slyB P2	A *	47 ± 1	13 ± 1
lpp	G	4 ± 1	3 ± 1
adk	G	8 ± 1	7 ± 1
trxA P1	U *	26 ± 1	24 ± 1
trxA P2	A	43 ± 2	11 ± 1
GlmY	A	33 ± 2	13 ± 1

The percentage of each transcript that was capped was determined by boronate gel electrophoresis and Northern blotting. Data from three biological replicates were used to calculate each mean and standard deviation.

*5′-terminal transcribed nucleotide of capped transcripts independently verified by 5′ RACE analysis of the capped fraction. All others are as reported (Kim et al., 2012).

Author Manuscript Author Manuscript Author Manuscript Author Manuscript

KEY RESOURCES TABLE

REAGENT or RESOURCE	SOURCE	IDENTIFIER
Bacterial and Virus Strains		
BW25113	Datsenko and Wanner, 2000	N/A
BW25113 Δ*apaH*	This study	N/A
BW25113 Δ*rppH*	Luciano et al., 2017	N/A
BW25113 Δ*apaH* Δ*rppH*	This study	N/A
BW25113 Δ*apaH* Δ*araE* Δ*araH*	This study	N/A
BW25113 Δ*apaH* Δ*rppH* Δ*araE* Δ*araH*	This study	N/A
BW25113 Δ*yeiP*	Luciano et al., 2017	N/A
BW25113 Δ*trxB*	Richards et al., 2012	N/A
BL21 (DE3) rne-131 Δ*rna*	This study	N/A
MIC2067	Itaya et al., 1999	N/A
Chemicals, Peptides, and Recombinant Proteins		
ApaH	This study	N/A
ApaH-D37A	This study	N/A
RppH	Foley et al., 2015	N/A
RppH-E53A	Foley et al., 2015	N/A
NudC	This study	N/A
NudC-E178A	This study	N/A
Tobacco acid pyrophosphatase	Epicentre	T19100
Pce1	Luciano et al., 2017	N/A
E. coli RNA polymerase	Nudler et al., 2003	N/A
LysU	This study	N/A
T7 RNA polymerase	Thermo Fisher	EP0111
T4 DNA ligase	Luciano et al., 2017	N/A
Calf intestinal alkaline phosphatase	New England Biolabs	M0290L
T4 polynucleotide kinase	New England Biolabs	M0201L
rRNasin	Promega	N251B
Inorganic pyrophosphatase	Sigma-Aldrich	I1643
T4 RNA ligase 1	New England Biolabs	M0204
SuperScript III reverse transcriptase	Thermo Fisher	18080-044
Nucleotides used in these studies	Table S7	N/A
Orthophosphoric acid, [^{32}P]	Perkin Elmer	NEX053S015MC
TALON Metal Affinity Resin	Clontech	635503
UNO Q1 column	Bio-Rad	7200001
TLC PEI cellulose F	Millipore	105579
3-acrylamidophenylboronic acid	Ivanov et al., 2004	N/A
Immobilon-Ny+	Millipore	INYC00010

Author Manuscript Author Manuscript Author Manuscript Author Manuscript

REAGENT or RESOURCE	SOURCE	IDENTIFIER
Sephadex G-25	GE Healthcare	17-0031-02
Phenol	Fisher Scientific	A92-500
Cadmium chloride		
Diamide	Sigma-Aldrich	D3648
L-arabinose	Sigma-Aldrich	A3256
Isopropyl β-D-1-thiogalactopyranoside (IPTG)	GoldBio	I2481
L-lysine	Sigma-Aldrich	L5626
Sucrose	Sigma-Aldrich	S0389
Rifampicin	Sigma-Aldrich	R3501
Oligonucleotides		
Oligonucleotides used in these studies	Table S7	N/A
Recombinant DNA		
Plasmids used in these studies	Table S7	N/A
Software and Algorithms		
ImageQuant TL	GE Healthcare	29000737
ciCalc2	This study	https://www.dropbox.com/sh/yni7ayej6iqz2mu/AADNwGYK__lnvwHHUDc_01d0a?dl=0